



This is a repository copy of *PIKfyve/Fab1 is required for efficient V-ATPase and hydrolase delivery to phagosomes, phagosomal killing, and restriction of Legionella infection.*

White Rose Research Online URL for this paper:
<http://eprints.whiterose.ac.uk/142934/>

Version: Published Version

Article:

Buckley, C.M. orcid.org/0000-0003-2105-0456, Heath, V.L., Guého, A. orcid.org/0000-0002-8992-8686 et al. (11 more authors) (2019) PIKfyve/Fab1 is required for efficient V-ATPase and hydrolase delivery to phagosomes, phagosomal killing, and restriction of Legionella infection. *PLoS Pathogens*, 15 (2). e1007551. ISSN 1553-7366

<https://doi.org/10.1371/journal.ppat.1007551>

Reuse

This article is distributed under the terms of the Creative Commons Attribution (CC BY) licence. This licence allows you to distribute, remix, tweak, and build upon the work, even commercially, as long as you credit the authors for the original work. More information and the full terms of the licence here:
<https://creativecommons.org/licenses/>

Takedown

If you consider content in White Rose Research Online to be in breach of UK law, please notify us by emailing eprints@whiterose.ac.uk including the URL of the record and the reason for the withdrawal request.



eprints@whiterose.ac.uk
<https://eprints.whiterose.ac.uk/>

RESEARCH ARTICLE

PIKfyve/Fab1 is required for efficient V-ATPase and hydrolase delivery to phagosomes, phagosomal killing, and restriction of *Legionella* infection

Catherine M. Buckley^{1,2^{aa}}, Victoria L. Heath³, Aurélie Guého⁴, Cristina Bosmani⁴, Paulina Knobloch⁵, Phumzile Sikakana¹, Nicolas Personnic⁵, Stephen K. Dove⁶, Robert H. Michell⁶, Roger Meier^{7^{ab}}, Hubert Hilbi⁵, Thierry Soldati⁴, Robert H. Insall^{8*}, Jason S. King^{1,2*}

1 Centre for Membrane Interactions and Dynamics, Department of Biomedical Sciences, University of Sheffield, Firth Court, Western Bank, Sheffield, United Kingdom, **2** Bateson Centre, University of Sheffield, Firth Court, Western Bank, Sheffield, United Kingdom, **3** Institute of Cardiovascular Sciences, Institute for Biomedical Research, College of Medical and Dental Sciences, University of Birmingham, Edgbaston, Birmingham, United Kingdom, **4** Department of Biochemistry, Faculty of Sciences, University of Geneva, Geneva, Switzerland, **5** Institute of Medical Microbiology, University of Zürich, Zürich, Switzerland, **6** School of Biosciences, University of Birmingham, Edgbaston, Birmingham, United Kingdom, **7** Institute of Molecular Life Sciences, University of Zürich, Zürich, Switzerland, **8** CRUK Beatson Institute, Switchback Road, Bearsden, Glasgow, United Kingdom

^{aa} Current address: Sick kids hospital for Sick Children, Toronto, Canada.

^{ab} Current address: Scientific Center for Optical and Electron Microscopy, ETH Zürich, Zürich, Switzerland

* R.Insall@beatson.gla.ac.uk (RHI); Jason.King@sheffield.ac.uk (JSK)



OPEN ACCESS

Citation: Buckley CM, Heath VL, Guého A, Bosmani C, Knobloch P, Sikakana P, et al. (2019) PIKfyve/Fab1 is required for efficient V-ATPase and hydrolase delivery to phagosomes, phagosomal killing, and restriction of *Legionella* infection. *PLoS Pathog* 15(2): e1007551. <https://doi.org/10.1371/journal.ppat.1007551>

Editor: Zhao-Qing Luo, Purdue University, UNITED STATES

Received: July 18, 2018

Accepted: January 3, 2019

Published: February 7, 2019

Copyright: © 2019 Buckley et al. This is an open access article distributed under the terms of the [Creative Commons Attribution License](https://creativecommons.org/licenses/by/4.0/), which permits unrestricted use, distribution, and reproduction in any medium, provided the original author and source are credited.

Data Availability Statement: All relevant data are within the paper and its Supporting Information files.

Funding: JSK is supported by a Royal Society University Research Fellowship UF140624. RHI is funded by Cancer Research UK Institute Group award A15672 and MRC grant G117/537. The Soldati laboratory is supported by multiple grants from the Swiss National Science Foundation (SNF) and TS is a member of iGE3 (<http://www.ige3>).

Abstract

By engulfing potentially harmful microbes, professional phagocytes are continually at risk from intracellular pathogens. To avoid becoming infected, the host must kill pathogens in the phagosome before they can escape or establish a survival niche. Here, we analyse the role of the phosphoinositide (PI) 5-kinase PIKfyve in phagosome maturation and killing, using the amoeba and model phagocyte *Dictyostelium discoideum*. PIKfyve plays important but poorly understood roles in vesicular trafficking by catalysing formation of the lipids phosphatidylinositol (3,5)-bisphosphate (PI(3,5)₂) and phosphatidylinositol-5-phosphate (PI(5)P). Here we show that its activity is essential during early phagosome maturation in *Dictyostelium*. Disruption of *PIKfyve* inhibited delivery of both the vacuolar V-ATPase and proteases, dramatically reducing the ability of cells to acidify newly formed phagosomes and digest their contents. Consequently, *PIKfyve*⁻ cells were unable to generate an effective antimicrobial environment and efficiently kill captured bacteria. Moreover, we demonstrate that cells lacking PIKfyve are more susceptible to infection by the intracellular pathogen *Legionella pneumophila*. We conclude that PIKfyve-catalysed phosphoinositide production plays a crucial and general role in ensuring early phagosomal maturation, protecting host cells from diverse pathogenic microbes.

unige.ch). HH is supported by the University of Zürich and the SNF (31003A_153200 and PZ00P3_161492). Microscopy studies were supported by a UK Medical Research Council grant (G0700091) and a Wellcome Trust grant (GR077544AIA). The funders had no role in study design, data collection and analysis, decision to publish, or preparation of the manuscript

Competing interests: The authors have declared that no competing interests exist.

Author summary

Cells that capture or eat bacteria must swiftly kill them to prevent pathogens from surviving long enough to escape the bactericidal pathway and establish an infection. This is achieved by the rapid delivery of components that produce an antimicrobial environment in the phagosome, the compartment containing the captured microbe. This is essential both for the function of immune cells and for amoebae that feed on bacteria in their environment. Here we identify a central component of the pathway used by cells to deliver antimicrobial components to the phagosome and show that bacteria survive over three times as long within the host if this pathway is disabled. We show that this is of general importance for killing a wide range of pathogenic and non-pathogenic bacteria, and that it is physiologically important if cells are to avoid infection by the opportunistic human pathogen *Legionella*.

Introduction

Professional phagocytes must kill their prey efficiently if they are to prevent the establishment of infections [1]. Multiple mechanisms are employed to achieve this. Once phagosomes have been internalised they quickly become acidified and acquire reactive oxygen species, antimicrobial peptides and acid hydrolases. The timely and regulated delivery of these components is vital to protect the host from intracellular pathogens but is incompletely understood.

After a particle is internalised, specific effector proteins are recruited to the phagosome's cytoplasmic surface by interacting with several inositol phospholipids (PIPs) that play important roles in regulating vesicle trafficking and controlling maturation. The effectors of each PIP regulate particular aspects of compartment identity, membrane trafficking and endosomal maturation [2, 3]. Phosphatidylinositol-3-phosphate (PI(3)P), made by the class III PI 3-kinase VPS34, is one of the first PIPs to accumulate on vesicles after endocytosis. PI(3)P recruits proteins containing FYVE (Fab1, YOTB, Vac1 and EEA1) and PX domains, such as the canonical early endosome markers EEA1 and Hrs, and sorting nexins [4, 5]. Also recruited to early endosomes by its FYVE domain is PIKfyve (Fab1 in yeast) [6], a phosphoinositide 5-kinase that phosphorylates PI(3)P to phosphatidylinositol-3,5-bisphosphate (PI(3,5)P₂) [7–11]. The roles of PI(3)P are well explored but the formation of PI(3,5)P₂ and the identities and functions of its effector proteins and its metabolic product PI(5)P are less well understood [12–14]. PI(3,5)P₂ is thought to accumulate predominantly on late endosomes, and disruption of PIKfyve activity leads to multiple endocytic defects, including gross endosomal enlargement and accumulation of autophagosomes [15–20]. Recent research has begun to reveal important physiological roles of PIKfyve and its products in a variety of eukaryotes, but mechanistic details remain sparse [21–25].

As in classical endocytosis, phagosome maturation is regulated by PIPs [26]. Phagosomes accumulate PI(3)P immediately after closure, and this is required for their subsequent maturation [27–29]. The recent identification of several PIKfyve inhibitors, including apilimod and YM201636 [30, 31], has allowed researchers to demonstrate the importance of PI(3)P to PI(3,5)P₂ conversion for phagosomal maturation in macrophages and neutrophils [32–35]. However, there are conflicting reports on the roles of PIKfyve in key lysosomal functions such as acidification and degradation, with some studies reporting defective acidification upon PIKfyve inhibition [10, 36, 37] and others finding little effect [33, 38, 39]. Therefore the mechanistic roles of PIKfyve and its products, and their relevance to phagosome maturation, remain unclear and subject to debate.

To understand the function and physiological significance of PIKfyve, we have investigated its role in phagosome maturation and pathogen killing in *Dictyostelium discoideum*, a soil-dwelling amoeba and professional phagocyte that feeds on bacteria. *Dictyostelium* PIPs are unusual, with the lipid chain joined to the *sn*-1-position of the glycerol backbone by an ether, rather than ester, linkage: these PIPs should correctly be named as derivatives of plasmalyngol rather than phosphatidylinositol [40]. This, however, makes no known difference to downstream functions, which are dictated by interactions between the inositol polyphosphate headgroups and effector proteins. *Dictyostelium* has thus been an effective model for analysis of phosphoinositide signalling [41–44]. For convenience, both the mammalian and *Dictyostelium* inositol phospholipids are referred to as PIPs hereafter.

We find that genetic or pharmacological disruption of PIKfyve activity in *Dictyostelium* leads to a swollen endosomal phenotype reminiscent of defects in macrophages. We provide a detailed analysis of phagosome maturation, and show that at least some of the defects in PIKfyve-deficient cells are due to reduced recruitment of the proton-pumping vacuolar (V-ATPase). Finally, we demonstrate that PIKfyve activity is required for the efficient killing of phagocytosed bacteria and for restricting the intracellular growth of the pathogen *Legionella pneumophila*.

Results

PIKfyve⁻ *Dictyostelium* have swollen endosomes

The *Dictyostelium* genome contains a single orthologue of *PIKfyve* (*PIP5K3*). Like the mammalian and yeast proteins, *Dictyostelium* PIKfyve contains an N-terminal FYVE domain, a CCT (chaperonin Cpn60/TCP1)-like chaperone domain, a PIKfyve-unique cysteine/histidine-rich domain and a C-terminal PIP kinase domain [7]. In order to investigate the role of PI(3,5)P₂ in *Dictyostelium* we disrupted the *PIKfyve* gene in the axenic Ax3 background by inserting a blasticidin resistance cassette and deleting a portion of the central PIKfyve-unique region. Gene disruption was confirmed by PCR of the genomic locus and loss of mRNA demonstrated by reverse transcription PCR (RT-PCR) (S1 Fig). Two independent mutants were isolated *PIKfyve-1* and *-2* (strain ID's JSK06 and JSK07 respectively).

While the unusual ether-linked chemistry of the *Dictyostelium* inositol phospholipids prevented direct measurement of PI(3,5)P₂ loss by either the standard method of methanolysis followed by HPLC of deacylation products or by mass spectrometry, we found that each mutant strain was highly vacuolated (Fig 1A and 1B), resembling the swollen vesicle phenotype observed upon *PIKfyve* knockdown or inhibition in mammalian cells, *C. elegans*, *S. cerevisiae* and *D. melanogaster* [10, 15, 20, 45]. This effect was recapitulated by incubation with the PIKfyve-specific inhibitor apilimod [30], confirming that this phenotype was due to deficient PIKfyve activity, most likely via the production of PI(3,5)P₂ or PI(5)P (Fig 1B).

The large vacuoles normally observable in axenically growing *Dictyostelium* are derived from either macropinocytic uptake of extracellular nutrients, or the contractile vacuole which aids osmoregulation by pumping water from the cytoplasm into specialised bladders for expulsion. To test if the swollen vesicles are macropinocytic in origin, cells were incubated with the fluid-phase marker TRITC-dextran for 2 hours. To further confirm macropinosome identity, we used cells expressing the PI(3)P reporter GFP-2xFYVE which specifically labels the early stages of this pathway ([46] and see later). Confocal microscopy showed that *PIKfyve*⁻ cells contained a dramatic increase in enlarged macropinosomes, at both early and late stages of maturation at a comparable size and number to the swollen vesicles described above (Fig 1A–1C). We therefore conclude that in *Dictyostelium*, the swollen vesicles observed upon loss of PIKfyve activity are macropinocytic in origin.

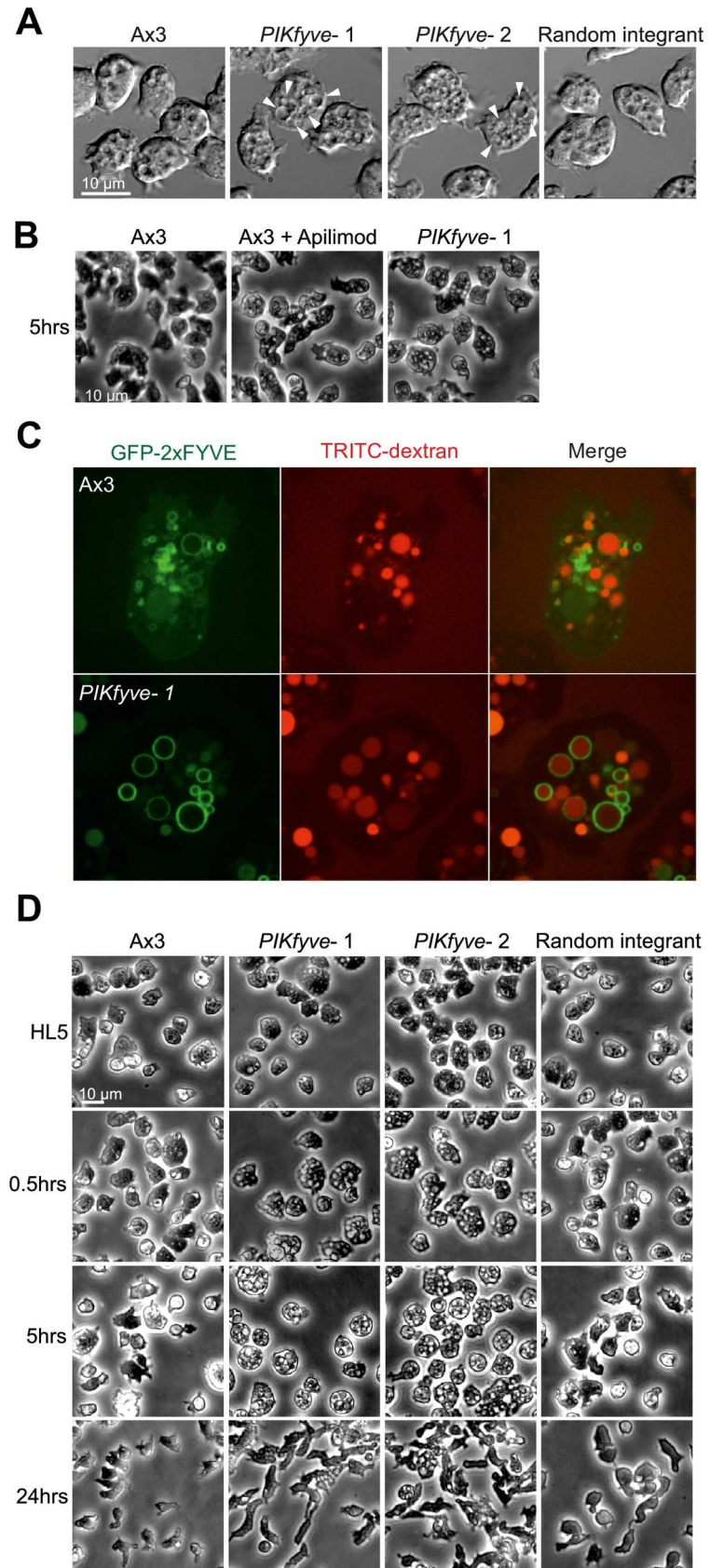


Fig 1. Knockout or inhibition of PIKfyve leads to a swollen vesicle phenotype. (A) DIC images of Ax3, two independent *PIKfyve*⁻ clones and a random integrant growing in HL5 medium. Arrows indicate the enlarged vesicles. (B) Induction of swollen vesicles with 5 μM apilimod, a PIKfyve-specific inhibitor, images taken in HL5 medium after 5 hours of treatment. (C) Confocal images of cells expressing the PI(3)P reporter GFP-2xFYVE. Cells were incubated with 0.2 mg/ml TRITC-dextran for 2 hours to label macropinosomes indicating that the swollen compartments in *PIKfyve*⁻ cells derive from this pathway. (D) Changes in morphology upon incubation in low osmolarity starvation buffer (KK2) compared to full medium (HL5). Swollen vesicles in *PIKfyve*⁻ cells became initially more apparent but were lost as cells entered differentiation.

<https://doi.org/10.1371/journal.ppat.1007551.g001>

When *PIKfyve*- amoebae were hypotonically stressed in phosphate buffer, we observed a sustained increase in vacuolation for at least 5 hours. However, after 24 hours—when the cells became polarized indicating the onset of starvation-induced development—*PIKfyve*- mutants became indistinguishable from the random integrant and parental controls (Fig 1D). This is most likely due to the suppression of fluid-phase uptake that occurs when *Dictyostelium* cells enter starvation-induced development [47–49]. Consistent with this interpretation, *PIKfyve*⁻ cells had no observable delay or other defects in development, and formed morphologically normal fruiting bodies with viable spores (S2 Fig). Therefore, disruption of PIKfyve leads to endocytic defects but it is not required for *Dictyostelium* development.

PIKfyve is important for phagocytic growth but not uptake

Laboratory strains of *Dictyostelium* can obtain nutrients by macropinocytosis of liquid (axenic) medium or by phagocytosis of bacteria. Although intracellular macropinosomes were swollen, *PIKfyve*⁻ cells had normal rates of both endocytosis and exocytosis (Fig 2A and 2B). Furthermore, the fluid uptake of both wild-type and *PIKfyve*-cells reached a plateau at about 60 minutes. This steady-state occurs when the first vesicles complete their transit and are exocytosed and indicates that the overall transit time in the absence of PIKfyve is unperturbed. Despite this, axenic growth was slower than for wild-type cells, with mutants doubling every 16 hours compared to 10 hours for the controls (Fig 2C).

Growth on bacteria was more strongly affected. When we measured phagocytosis by following the ability of *Dictyostelium* cells to decrease the turbidity of an *E. coli* suspension over time we found no significant defects in *PIKfyve*⁻ cells (Fig 2D). In contrast, they grew significantly more slowly on a lawn of *Klebsiella pneumoniae* (Fig 2E). This indicates a specific role for PIKfyve activity in phagosome maturation rather than bacterial uptake.

PIKfyve deficient cells have defective phagosome acidification and V-ATPase delivery

Next we investigated how the absence of PIKfyve affects phagosomal maturation. One of the first stages of maturation is the acquisition of the proton-pumping V-ATPase, leading to rapid acidification [50, 51]. The influence of PIKfyve on endosomal pH regulation remains controversial: studies in *C. elegans*, plants, and mammalian epithelial cells have shown that PIKfyve is required for efficient acidification [37, 45, 52–54], but RAW 264.7 macrophages are still able to acidify their phagosomes to at least pH 5.5 when treated with a PIKfyve inhibitor [33].

Phagosome maturation is well characterised in *Dictyostelium*, with most studies being performed using mutants in the Ax2 genetic background, rather than Ax3 as used above. For comparison with other studies we isolated additional mutants from Ax2 cells, which were used for all subsequent experiments unless stated otherwise. Ax2 background *PIKfyve* mutants also exhibited slow growth on bacterial lawns but normal phagocytosis of both beads and bacteria (S3 Fig), confirming that these phenotypes are robust across multiple genetic backgrounds.

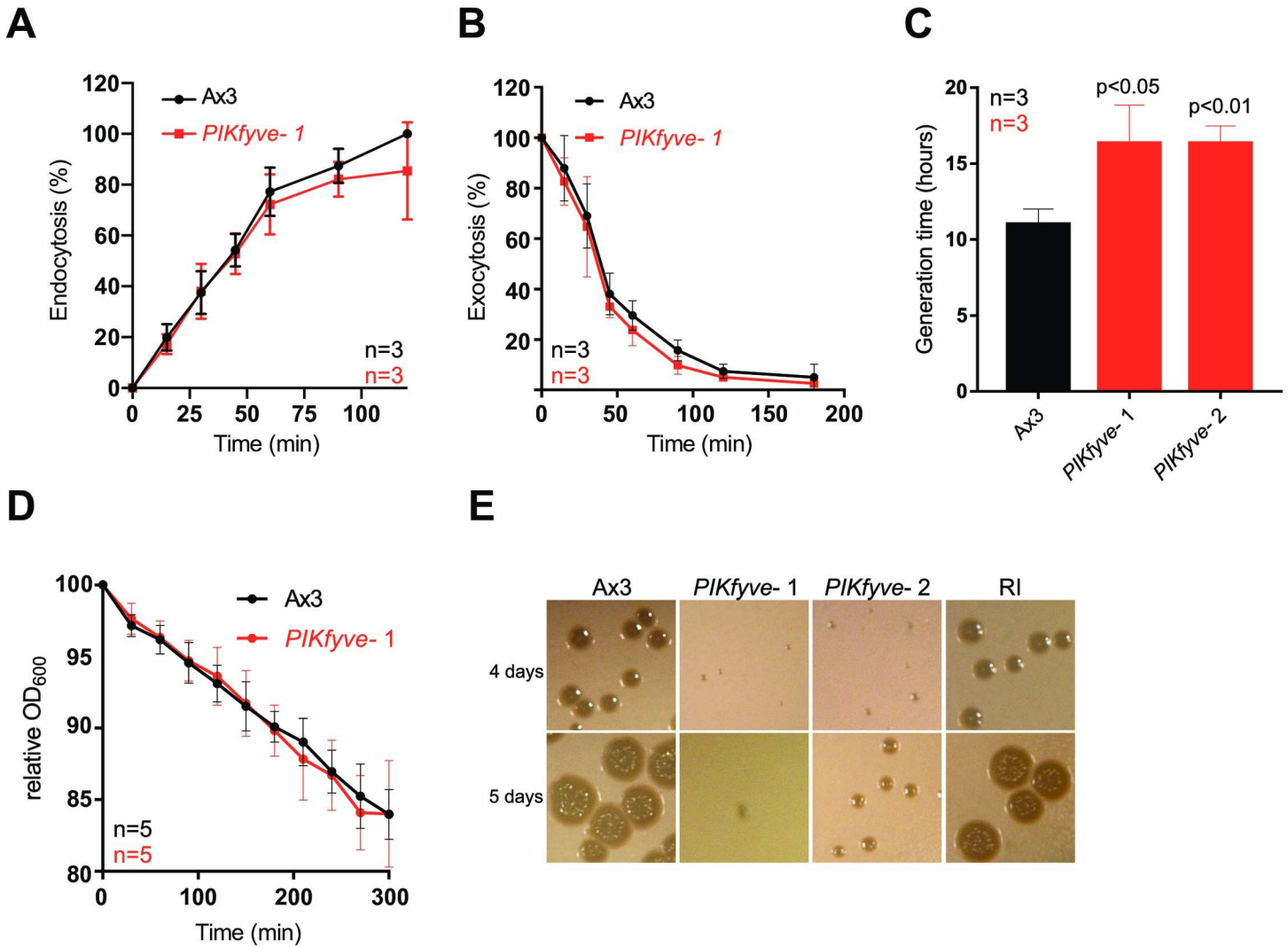


Fig 2. *PIKfyve*-null cells have growth defects. Measurement of (A) macropinocytosis or (B) exocytosis in Ax3 and *PIKfyve*⁻ cells as measured by uptake or loss of FITC dextran. (C) Growth rates in axenic culture. *PIKfyve*⁻ cells had a significantly longer generation time than Ax3 cells (Student's t-test). (D) Phagocytosis of *E. coli*, as measured by the ability of *Dictyostelium* cells to reduce the turbidity of a bacterial suspension. (E) Growth of *PIKfyve* mutants on lawns of *K. pneumoniae* as indicated by the clearance of bacteria-free plaques on agar plates. RI denotes a random integrant control. All data plotted are mean \pm SD.

<https://doi.org/10.1371/journal.ppat.1007551.g002>

We followed phagosome acidification in *PIKfyve*⁻ *Dictyostelium* by measuring changes in the relative fluorescence of engulfed beads that had been labelled both with the pH-sensitive FITC and the pH-insensitive Alexa 594 succinimidyl ester [55]. Phagosomes from wild-type cells rapidly became acidified and remained acidic until ~40 minutes before transitioning to neutral post-lysosomes, but phagosomes of *PIKfyve*⁻ cells acidified much more slowly and never achieved as low a pH (Fig 3A). In contrast, when we incubated cells with a mixture of FITC- and pH-insensitive TRITC-conjugated dextrans to observe the acidification of macropinosomes, we found that they were still able to acidify sufficiently to quench FITC fluorescence (S4 Fig). However the concentration of dextrans within macropinosomes did appear delayed. This is consistent with the relatively mild defect in axenic growth and previous studies in mammalian cells [38], indicating a more stringent requirement for PIKfyve activity during phagosome acidification.

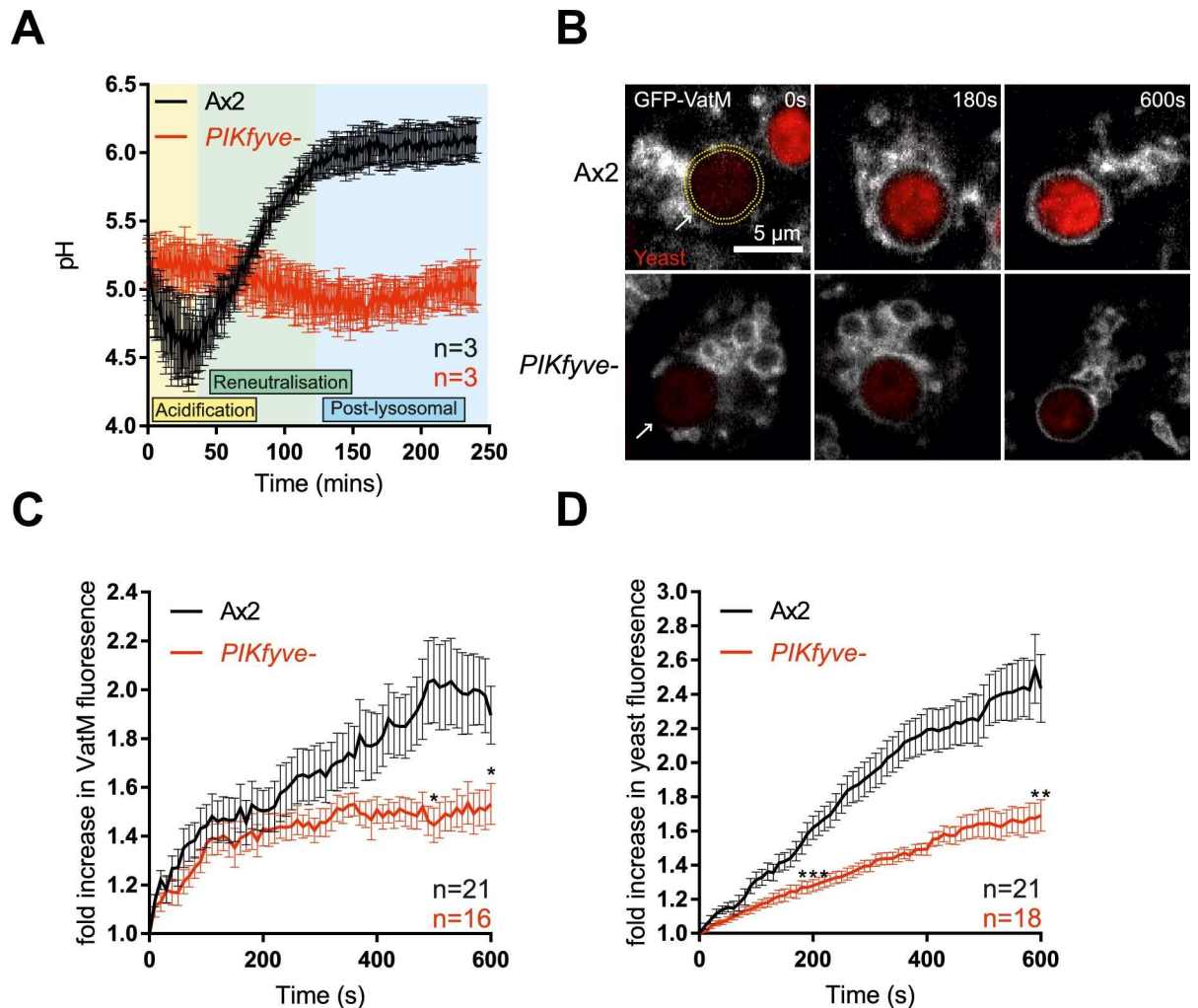


Fig 3. Disruption of *PIKfyve* reduces V-ATPase delivery and phagosome acidification. (A) Measurement of phagosomal acidification in Ax2 and *PIKfyve*⁻ cells after engulfment of beads conjugated to pH-sensitive fluorophores. After initial acidification, *Dictyostelium* phagosomes reneutralise ~45 minutes prior to exocytosis. (B) Recruitment of the V-ATPase subunit GFP-VatM to phagocytosed pHrodo-labelled yeast visualised by confocal time-lapse imaging. (C) Quantification of GFP-VatM recruitment over time averaged across multiple phagocytic events. Images were quantified by automated selection of a 0.5 μm-thick ring surrounding the yeast at each time point (see yellow dotted circle in (B)). N indicates the total number of cells analysed over 3 independent experiments. Quantification of the associated increase in yeast-associated pHrodo fluorescence, indicating acidification is shown in (D). Data shown are mean +/- SEM, p values calculated by Student's t-test: *p<0.05, **p<0.01, ***p<0.005.

<https://doi.org/10.1371/journal.ppat.1007551.g003>

Phagosomal acidification is driven by the rapid recruitment and activity of the V-ATPase. To differentiate between defective V-ATPase delivery and activity, we directly imaged recruitment of the VatM transmembrane subunit of the V-ATPase fused to GFP to nascent phagosomes by microscopy. By observing the phagocytosis of pH-sensitive pHrodo-labelled yeast we were able to simultaneously monitor acidification.

GFP-VatM began accumulating on phagosomes immediately following internalisation both in *PIKfyve*⁻ and control cells, but it accumulated more slowly in the mutants and to only about half of the levels observed in wild-type cells (Fig 3B and 3C). Defective acidification was further demonstrated by a reduced increase in pHrodo fluorescence (Fig 3D). We conclude that there is some *PIKfyve*-independent lysosomal fusion with phagosomes, but that *PIKfyve*

activity is required for the high levels of V-ATPase accumulation that are needed for efficient phagosomal acidification.

The V-ATPase consists of V_0 (transmembrane) and V_1 (peripheral) subcomplexes. It has previously been suggested that PI(3,5)P₂ can regulate V_0 - V_1 assembly at the yeast vacuole allowing dynamic regulation of activity [56]. VatM is a component of the V_0 subcomplex (subunit a in mammals and yeast). To test whether V_0 - V_1 association is also affected by loss of PIKfyve we observed the phagosomal recruitment of the V_1 subunit VatB fused to GFP [57]. Both GFP-VatM and VatB-GFP were expressed equally in wild-type and mutant cells (S5A Fig). As before VatB-GFP recruitment to nascent phagosomes was also significantly decreased in *PIKfyve*⁻ cells (S5B and S5C Fig)

It should be noted that expression of VatB-GFP (but not GFP-VatM) caused a partial inhibition of acidification in this assay, indicating caution should be taken in using this construct (S5D Fig). Nevertheless, the observation that both V-ATPase components were equally affected by PIKfyve deletion suggests that PIKfyve is required for delivery of the entire V-ATPase to the phagosome, rather than specifically affecting V_0 - V_1 association.

Proteolytic activity and hydrolase delivery are specifically affected in *PIKfyve*⁻ cells

Proper degradation of internalised material requires both acidification and the activity of proteases. To test if hydrolytic activity was also dependent on PIKfyve, we measured phagosomal proteolysis by following the increase in fluorescence due to the cleavage and unquenching of DQ-bovine serum albumin (DQ-BSA) coupled to beads [55] (Fig 4A). Strikingly, despite their partial acidification, phagosomes in *PIKfyve*⁻ cells exhibited an almost complete loss of proteolytic activity, an effect confirmed using the PIKfyve inhibitor apilimod (S6 Fig). To control for a potential general decrease in protease activity, we measured the unquenching of DQ-BSA beads in whole cell lysates (Fig 4B) and the protein levels of lysosomal protease cathepsin D by Western blot (Fig 4C and 4D). Although activity in the phagosome is completely lost, we found that total proteolytic activity remained normal and cathepsin D levels were significantly increased upon loss of *PIKfyve*, consistent with a defect in delivery to the phagosome, rather than in lysosomal biogenesis.

To investigate whether PIKfyve activity was required to deliver proteases to the phagosome, we purified phagosomes at different stages of maturation and analysed their composition by Western blot (Fig 4E). In wild-type cells phagosomes acquired cathepsin D from the earliest time-point, but the protease was almost completely absent from phagosomes in *PIKfyve*⁻ cells. Whilst the delivery of the vacuolar ATPase was also qualitatively reduced in this assay, consistent with decreased acidification, Actin-binding protein 1 (Abp1), an independent marker of phagosome maturation [58], was unaffected. Thus, although both hydrolase and to a lesser extent V-ATPase delivery requires PIKfyve activity, other aspects of maturation appear to progress normally.

PIKfyve does not regulate PI(3)P dynamics

We next wanted to confirm whether loss of PIKfyve disrupts specific aspects of phagosome maturation or causes a general trafficking defect. PI(3)P is one of the best characterised early markers of maturing endosomes and phagosomes in both mammalian macrophages and *Dictyostelium*. Immediately following particle internalization, PI(3)P is generated on the phagosome by the class III PI 3-kinase VPS34 [27, 33, 46] and interacts with a number of important regulators of maturation such as Rab5 [59]. PIKfyve is both recruited by PI(3)P and phosphorylates it, forming PI(3,5)P₂. Loss of PIKfyve activity could perturb phagosome maturation by

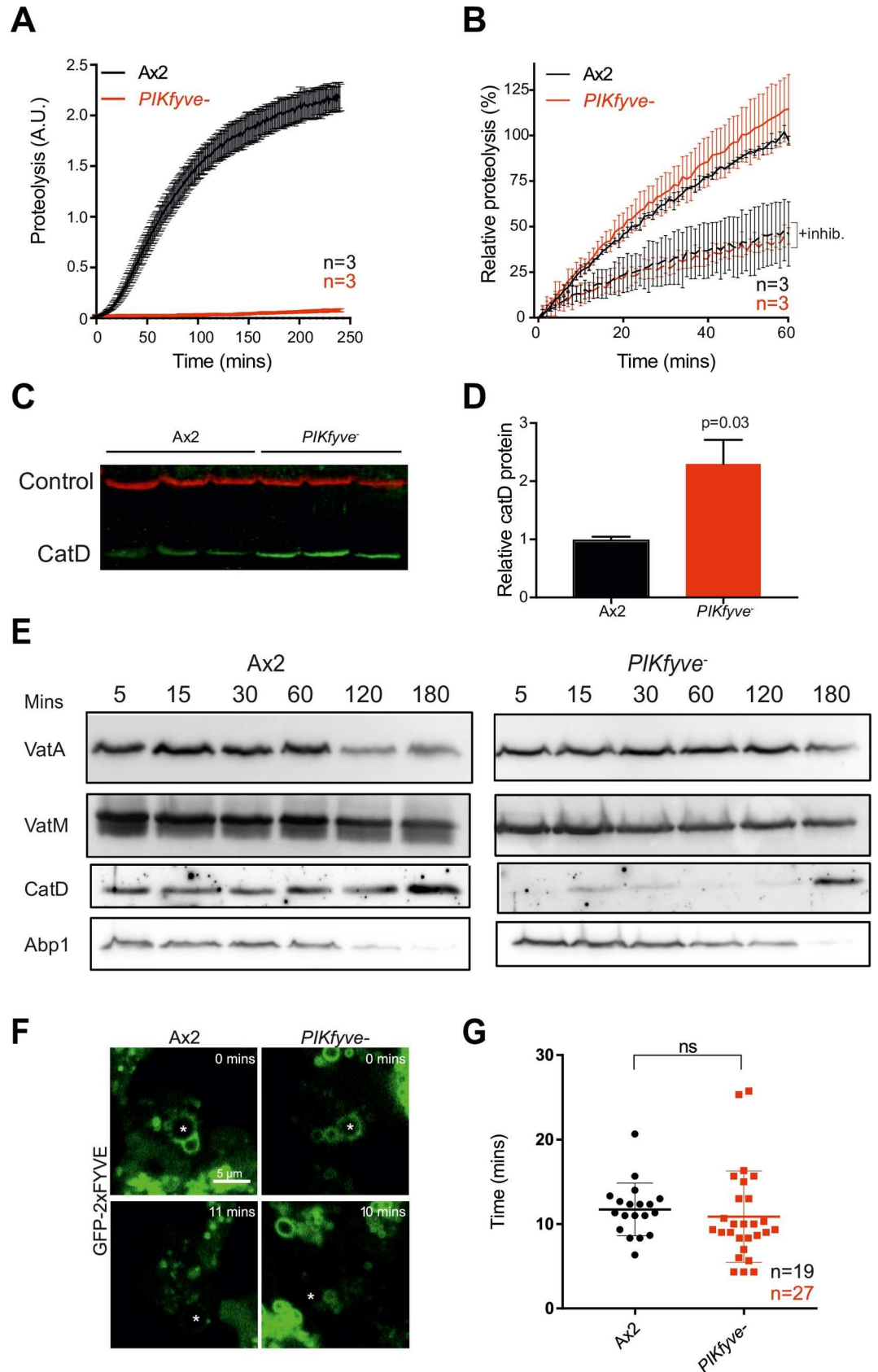


Fig 4. PIKfyve is required for hydrolase activity and proteolysis. (A) Phagosomal proteolysis measured by dequenching of DQ-BSA-conjugated beads after phagocytosis. (B) Total proteolytic activity in cell lysates against DQ-BSA-beads is unchanged upon *PIKfyve* disruption, dotted lines are parallel samples in the presence of protease inhibitors. (C) Western blot of cathepsin D protein levels, three independent samples of each strain were normalised for total protein and are quantified in (D). Loading control is fluorescent streptavidin which recognises the mitochondrial protein MCCC1; P-value from a one-sample T-test. (E) Analysis of phagosome maturation, by purifying phagosomes from cells after maturation for the indicated times. VatA is a subunit of the V_1 subcomplex of the V-ATPase, whereas VatM is a V_0 component. Blots are from the same samples and are representative of multiple independent purifications. (F) Analysis of PI(3)P dynamics in the absence of PIKfyve. PI(3)P was monitored by the recruitment of GFP-2xFYVE following phagocytosis of 3 μ m beads (asterisks) imaged by confocal time-lapse microscopy. (G) Time that GFP-2xFYVE stays associated with phagosomes following engulfment, indicating that PI(3)P removal is not PIKfyve-dependent. N indicates the total number of cells quantified across 3 independent experiments. Data shown are mean \pm SEM (A & B) or SD (G).

<https://doi.org/10.1371/journal.ppat.1007551.g004>

reducing PI(3)P consumption, by eliminating the actions of PI(3,5)P₂, or both. Studies on macrophages have indicated that inhibition of PIKfyve can cause prolonged PI(3)P signalling [33].

PI(3)P can be visualised in cells using the well-characterised reporter GFP-2xFYVE [41, 60]. Expression of GFP-2xFYVE in control cells demonstrated that PI(3)P is present on *Dictyostelium* phagosomes immediately following engulfment, consistent with previous reports [46] (Fig 4F). However, we found no abnormalities in either the recruitment to or the dissociation from phagosomes of this reporter in *PIKfyve*⁻ mutants (Fig 4F and 4G). PIKfyve activity seems not to influence the steady-state levels of PI(3)P in *Dictyostelium*, and the functional defects in *PIKfyve*⁻ cells therefore are likely to be caused by a lack of the product(s) of PIKfyve activity.

Overall, the normal transition of *PIKfyve*⁻ phagosomes into a PI(3)P-negative compartment indicates that much of their phagosome maturation process continues normally—but with the product(s) of PIKfyve action playing specific role(s) in the delivery of certain important components, including the V-ATPase and hydrolytic enzymes.

PIKfyve is essential for efficient killing of bacteria

Acidification and proteolysis are important mechanisms used by phagocytes to kill engulfed microbes. We therefore asked whether PIKfyve was physiologically important for killing. Bacterial death leads to membrane permeabilisation and intracellular acidification, so survival time within phagosomes can be inferred by observing the phagocytosis and subsequent quenching of GFP fluorescence when expressed by a non-pathogenic *Klebsiella pneumoniae* strain [61]. In this assay, the phagocytosed bacteria survived more than three times longer in *PIKfyve*⁻ cells (median survival 12 min) than in wild-type cells (3.5 min) (Fig 5A and 5B). This effect was again recapitulated by treatment with 5 μ M apilimod (S6 Fig). These benign bacteria did eventually die in *PIKfyve*⁻ cells, indicating either that the residual acidification is eventually sufficient or that enough other elements of the complex bacterial killing machinery remain functional in *PIKfyve*⁻ phagosomes.

These defects in bacterial killing and digestion (Fig 4) explain why PIKfyve is important for *Dictyostelium* to grow on a lawn of *K. pneumoniae* (Fig 2E). To test whether this is general to a broad range of bacteria, we employed an assay whereby serial dilutions of amoebae are plated on lawns of a panel including both Gram-positive and Gram-negative bacteria [62]. In this assay, *PIKfyve*⁻ deficient cells were severely inhibited in growth on all bacteria tested, demonstrating a general role for PIKfyve in bacterial killing and digestion (Fig 5C and 5D).

PIKfyve activity restricts the persistence of *Legionella* infection

Many pathogenic bacteria infect host immune cells by manipulating phagosome maturation to establish a replication-permissive niche or to escape into the cytosol. To avoid infection, host

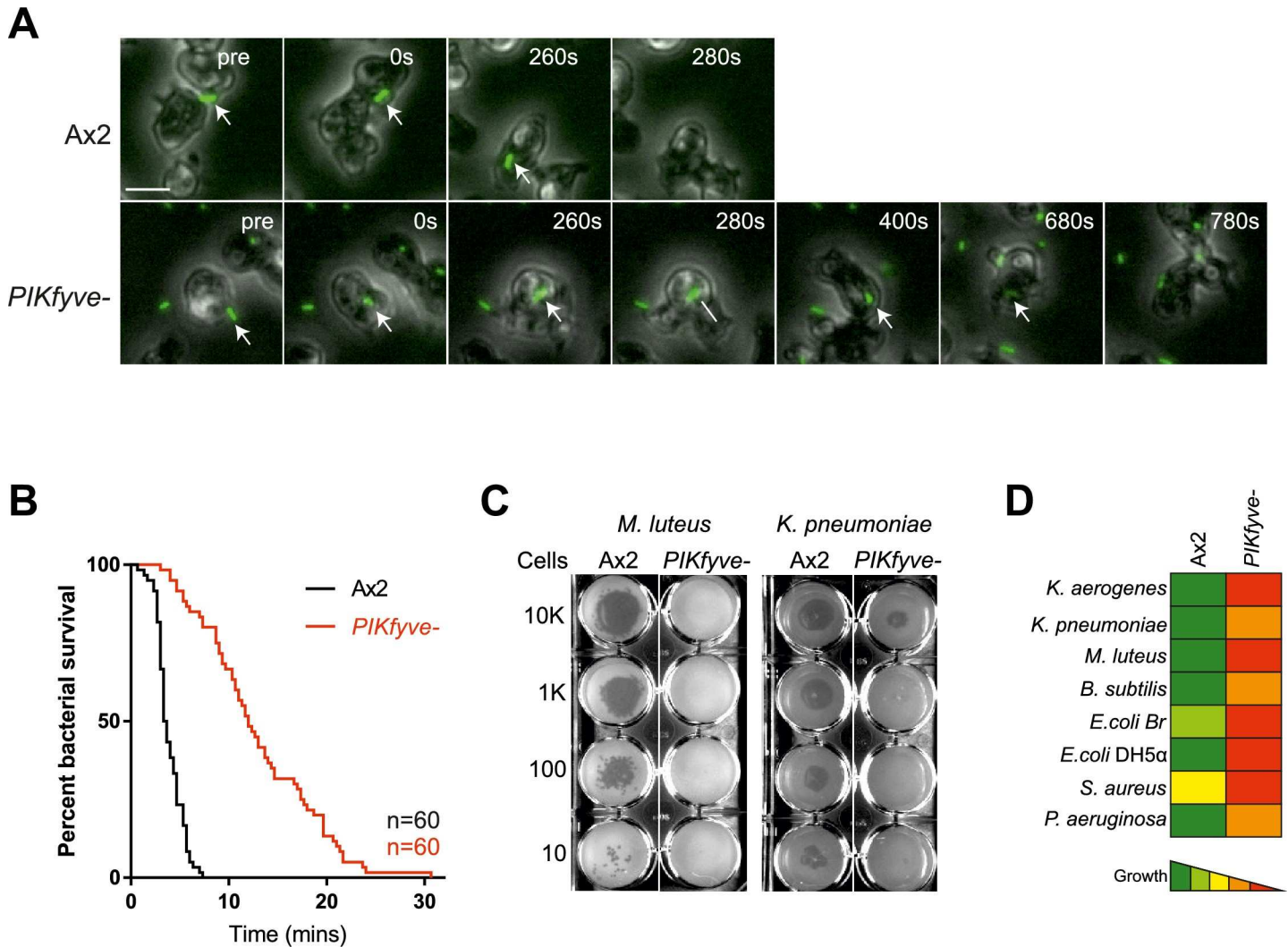


Fig 5. Bacterial survival is increased in *PIKfyve*-null cells. (A) Stills from widefield timelapse movies of *Dictyostelium* cells eating GFP-expressing *Klebsiella pneumoniae*. The point of bacterial cell permeabilisation and death can be inferred from the quenching of GFP fluorescence after engulfment. Arrows indicate captured bacteria. This is quantified in (B) which shows a Kaplan-Meier survival graph, based on the persistence of bacteria GFP-fluorescence within the amoebae. 60 bacteria were followed across three independent experiments and survived significantly longer in *PIKfyve*-null cells than Ax2 ($p < 0.0001$, Mantel-Cox test). (C) Loss of *PIKfyve* inhibits growth on diverse bacteria. Growth was assessed by plating serial dilutions of amoebae on lawns of different bacteria and dark plaques indicate amoebae growth. Data for all bacteria are summarised in (D).

<https://doi.org/10.1371/journal.ppat.1007551.g005>

cells must efficiently kill such pathogens; hence *PIKfyve* might be critical to protect host cells from infection.

Legionella pneumophila is a Gram-negative opportunistic human pathogen that normally lives in the environment by establishing replicative niches inside amoebae such as *Acanthamoeba*. This process can be replicated in the laboratory using *Dictyostelium* as an experimental host [63]. Following its phagocytosis, *Legionella* can disrupt normal phagosomal maturation and form a unique *Legionella*-containing vacuole (LCV). This requires the Icm/Dot (Intracellular multiplication/Defective for organelle trafficking) type IV secretion system that delivers a large number of bacterial effector proteins into the host (reviewed in [64]). These effectors modify many host signalling and trafficking pathways, one of which prevents the nascent *Legionella*-containing phagosome from fusing with lysosomes [65].

Phosphoinositide signalling is heavily implicated in *Legionella* pathogenesis, with *Legionella*-containing phagosomes rapidly accumulating PI(3)P. Its concentration then declines within 2 hours and PI(4)P accumulates [66]. Multiple effectors introduced through the Icm/Dot system bind PI(3)P or PI(4)P [67–73]. The role of PI(3,5)P₂ (and/or PI(5)P) in *Legionella* infection is yet to be investigated, so we tested whether PIKfyve was beneficial or detrimental for the host to restrain *Legionella* infection.

When we measured the rate of uptake of GFP-expressing *Legionella* by flow cytometry, we found PIKfyve⁻ *Dictyostelium* were indistinguishable from wild-type. Both strains phagocytosed many more of the virulent wild-type *Legionella* strain (JR32) than an avirulent strain that is defective in type IV secretion ($\Delta icmT$) [74] (Fig 6A). These results are in agreement with the previous finding that expression of the Icm/Dot T4SS promotes uptake of *Legionella* [75]. When we measured the ability of *Dictyostelium* to kill *Legionella* $\Delta icmT$, the bacteria survived for significantly longer in PIKfyve⁻ cells (Fig 6B).

We next tested the role of PIKfyve on the outcome of infection. When Ax2 and PIKfyve mutants were infected with either wild-type or $\Delta icmT$ *Legionella*, using a MOI of 0.1 to compensate for the greater uptake of wild-type *Legionella*, both amoeba strains suppressed the avirulent bacteria, although the reduction in bacteria was slower in the PIKfyve mutants. In contrast, wild-type *Legionella* grew substantially faster in cells lacking PIKfyve (Fig 6C, note that the CFUs scales in Fig 6B and 6C are logarithmic). We independently confirmed these results using flow cytometry of cells infected with GFP-producing bacteria in our Ax3-background mutants. The only *Dictyostelium* cells that accumulated substantial GFP fluorescence over several days were those infected by wild-type *Legionella*, and this happened sooner and to a greater degree in the PIKfyve⁻ cells (Fig 6D).

Unlike PI(3)P and PI(4)P, the lipid products of PIKfyve are thus not required for *Legionella* to subvert phagosome maturation and generate its replicative vacuole. Rather, the role of PIKfyve in ensuring rapid phagosomal acidification and digestion is crucial for the host to prevent *Legionella*, and presumably other pathogens, from surviving and establishing a permissive niche.

Discussion

In this study, we have characterised the role of PIKfyve during phagosome maturation using the model phagocyte *Dictyostelium*. The roles of PI 3-kinases and PI(3)P signalling during phagosome formation and early maturation have been studied extensively but the subsequent actions of PIKfyve and roles of PI(3,5)P₂ and PI(5)P are much less well understood [3, 26]. In non-phagocytic cells such as fibroblasts and yeast, PI(3,5)P₂ production is important for endosomal fission and fragmentation of endolysosomal compartments [10, 18, 37, 45], and PIKfyve inhibition has been shown to cause macrophage lysosomes to coalesce by an unknown mechanism [34]. PIKfyve also regulates macropinosome maturation [38], intracellular replication of the vaccinia virus and *Salmonella* [38, 53, 76] and production of reactive oxygen species (ROS) in neutrophils [35]. In this paper we show that PIKfyve is critical to ensure efficient phagosomal acidification and proteolysis via delivery of specific components, and we demonstrate its physiological importance in the killing of bacteria and suppression of intracellular pathogens.

Complex effects of PIKfyve inhibition on PIP-mediated signalling have hampered clear interpretation of PIKfyve function in some mammalian studies. For example, some studies report that disruption of PIKfyve both prolonged PI(3)P-mediated signalling and eliminated PI(3,5)P₂ production [30, 32], making it difficult to determine which phosphoinositide change is responsible for the observed phenotypes. In contrast, and in agreement with other reports in mammalian cells [18, 37], we found that deletion of PIKfyve had no impact on phagosomal PI

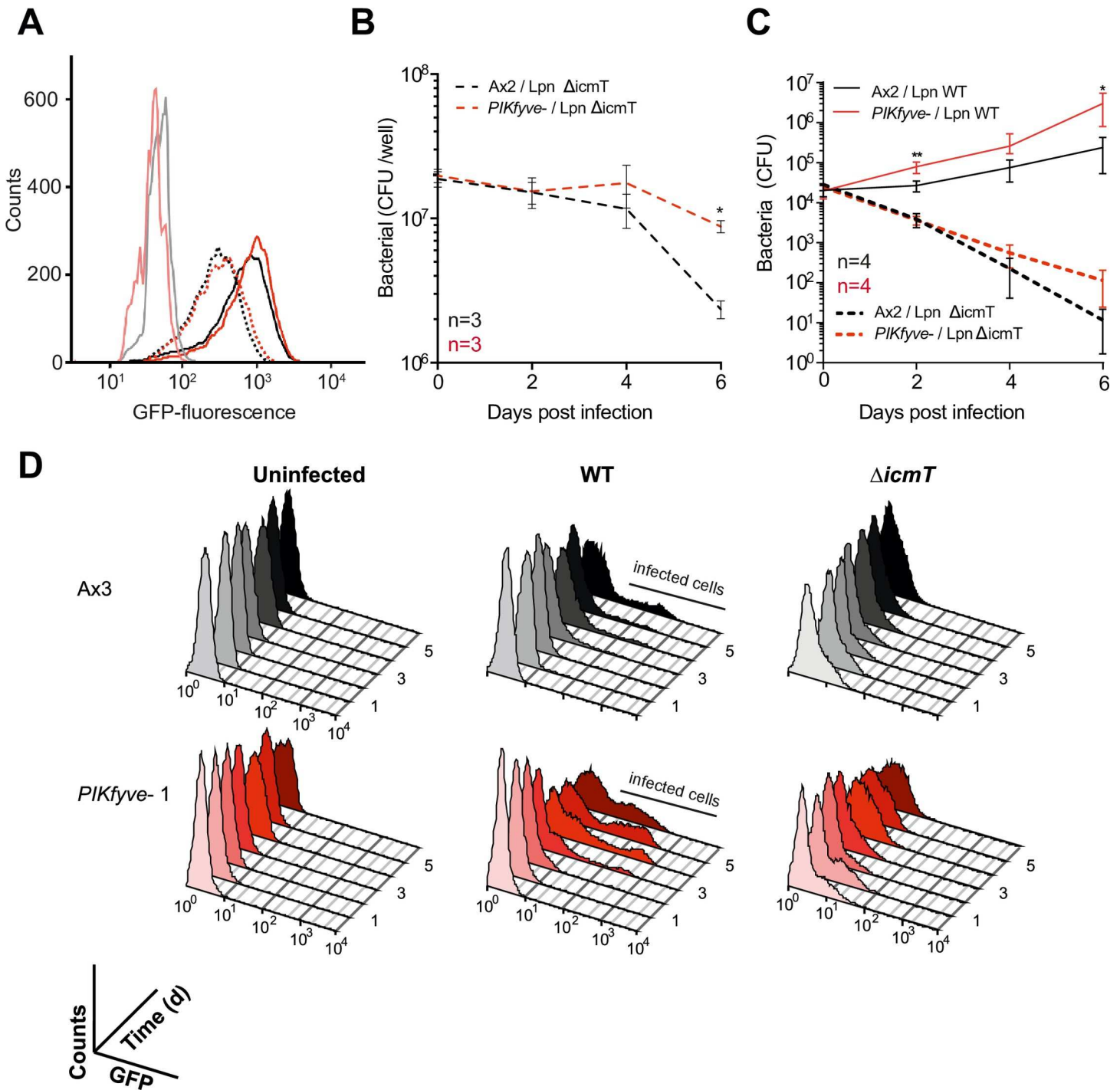


Fig 6. PIKfyve is required to suppress *Legionella* replication. A) Wild-type (Ax2, black lines), or *PIKfyve*-null *Dictyostelium* (red lines) were infected (MOI 50) with wild-type (JR32, solid lines) or avirulent ($\Delta icmT$, dotted lines) *Legionella* expressing GFP and fixed 40 min post infection before analysis by flow cytometry. The GFP fluorescence intensity, indicating bacteria per cell was indistinguishable between the two *Dictyostelium* strains, but higher for JR32 than $\Delta icmT$. Uninfected cells are represented by pale black/red lines. Data are representative of three independent experiments, performed in duplicate. (B) Survival of GFP- $\Delta icmT$ *Legionella* after infecting Ax2 and *PIKfyve*-null amoebae (MOI 50). Bacterial colony forming units (CFU) were determined at each timepoint after lysis of the *Dictyostelium* amoebae. (C) Outcome of infection with either wild-type (solid lines) or $\Delta icmT$ (dashed lines) *Legionella*. *Dictyostelium* cells were infected at a MOI of 0.1, and intracellular growth measured by CFU's at each indicated time. Data shown are the means \pm SEM of 3 independent experiments performed in triplicate (* = $p < 0.05$, ** $p < 0.01$ Student's t-test vs equivalent Ax2 infection). (D) Flow cytometry of intracellular bacterial burden of Ax3-derived *PIKfyve*-null cells infected with GFP-producing *Legionella* strains over time. Virulent *Legionella* replicate more efficiently in *PIKfyve*-*Dictyostelium*, as indicated by the increasing proportions of amoebae containing high levels of GFP over time. Graphs show $>10,000$ cells measured at each time point, and are representative of 3 independent experiments.

<https://doi.org/10.1371/journal.ppat.1007551.g006>

(3)P dynamics in *Dictyostelium*. The defects in phagosome maturation that we observed in this system are thus due to lack of PI(3,5)P₂/PI(5)P formation and not to prolonged PI(3)P signalling. There is limited evidence that PIKfyve might exhibit protein kinase activity [77], but whether this is relevant *in vivo* remains to be shown.

Whilst PIKfyve appears to be the major route of PI(3,5)P₂ synthesis, there remains the caveat that other pathways exist in *Dictyostelium* or mammalian cells. Indeed 20% of PI(3,5)P₂ levels remain after PIKfyve inhibition in fibroblasts [37] and whilst inhibition may not be complete it is also theoretically possible that a pool of PI(3,5)P₂ can be generated by 5-dephosphorylation of PIP₃, or 3-phosphorylation of PI(5)P. Whilst PIKfyve is the only route for PI(3,5)P₂ synthesis in yeast, until we are able to specifically measure PI(3,5)P₂ in *Dictyostelium* it is possible that alternative pathways exist.

The role of PIKfyve in lysosomal acidification and degradation is currently disputed. Several studies which have measured vesicular pH at a single time point have shown that PIKfyve is required for acidification [10, 37, 45, 54], whereas others found that disruption of PIKfyve had little effect on phagosomal pH [33, 38, 39]. In contrast, we followed the temporal dynamics of V-ATPase delivery and of phagosomal acidification and proteolysis, and showed that V-ATPase delivery to PIKfyve-deficient phagosomes was substantially decreased and delayed, with consequent defects on initial acidification and proteolysis. PI(3,5)P₂ has also been proposed to regulate V-ATPase V₀-V₁ subcomplex association dynamically at the yeast vacuole [56], but we found no evidence for this during *Dictyostelium* phagosome maturation.

It is still not clear how PIKfyve-generated PI(3,5)P₂ regulates V-ATPase trafficking, and few PI(3,5)P₂ effectors are known. One of these is the lysosomal cation channel TRPML1/mucolipin, which is specifically activated by PI(3,5)P₂ [78]. This interaction was recently shown to partly underlie the role of PIKfyve in macropinosome fragmentation, although not acidification [38]. TRPML1 is also required for phagosome-lysosome fusion [79], and PI(3,5)P₂ and TRPML1 have been proposed to mediate interactions between lysosomes and microtubules [80]. PIKfyve may therefore drive V-ATPase delivery to phagosomes both by microtubule-directed trafficking and by regulating fission. However, the sole mucolipin orthologue in *Dictyostelium* is only recruited to phagosomes much later, during the post-lysosomal phase, and its disruption influences exocytosis rather than acidification [81].

Effective phagosomal acidification and proteolysis is essential if phagocytes are to kill internalised bacteria. Many clinically relevant opportunistic pathogens, including *Legionella* [64, 82], *Burkholderia cenocepacia* [83] and *Cryptococcus neoformans* [84], have developed the ability to subvert normal phagosome maturation so as to maintain a permissive niche inside host phagocytes. This ability is likely to have evolved from their ancestors' interactions with environmental predators such as amoebae [85–87].

Legionella are phagocytosed in the lung by alveolar macrophages. After internalisation, they employ effectors secreted via their Type IV secretion system, some of which interfere with PI(3)P-signalling, to inhibit phagosome maturation [68, 88, 89]. We have shown that the products of PIKfyve are not required for *Legionella* to establish an intracellular replication niche. Rather, *Legionella* survive much better in PIKfyve-deficient cells, suggesting that PI(3,5)P₂ helps *Dictyostelium* to eliminate rather than harbour *Legionella*. Consistent with this, recent studies have shown that the *Legionella* virulence effector SidK directly binds to and suppresses the activity of the phagosomal V-ATPase, further underlining the importance of acidification in restricting pathogen survival [90, 91].

This is in contrast to the non-phagocytic invasion of epithelia that occurs during *Salmonella* infection. In that case, PIKfyve activity is necessary to promote the generation of a specialised survival niche within which the bacteria replicate [53]. *Salmonella* has thus evolved a specific requirement for PIKfyve in generating a survival niche—likely through using phagosome

acidification as a cue for virulence factor expression—whereas *Legionella* and other bacteria are suppressed by rapid and PIKfyve-driven phagosomal maturation.

The molecular arms race between host and pathogens is complex and of great importance. The very early events of phagosome maturation are critical in this competition; host cells aim to kill their prey swiftly whilst pathogens try to survive long enough to escape. Although its molecular effectors remain unclear, PIKfyve and its products are crucial to tip the balance in favour of the host, providing a general mechanism to ensure efficient antimicrobial activity.

Materials and methods

Cell strains and culture

Dictyostelium discoideum cells were grown in adherent culture in plastic Petri dishes in HL5 medium (Formedium) at 22°C. *PIKfyve*⁻ mutants were generated in both Ax2 and Ax3 backgrounds, with appropriate wild-type controls used in each case. Cells were transformed by electroporation and transformants selected in 20 µg/ml hygromycin (Invitrogen), 10 µg/ml G418 (Sigma) or 10 µg/ml blasticidin S. Apilimod was from United States Biological.

Growth in liquid culture was measured by seeding log phase cells in a 6 well plate and counting cells every 12 hours using a haemocytometer. Growth on bacteria was determined by plating ~10 *Dictyostelium* cells on SM agar plates (Formedium) spread with a lawn of non-pathogenic KpGe *K. pneumoniae* [92].

Plaque assays were performed as previously described [93]. Briefly, serial dilution of *Dictyostelium* cells (10–10⁴) were placed on bacterial lawns and grown until visible colonies were obtained. The bacterial strains were kindly provided by Pierre Cosson and were: *K. pneumoniae* laboratory strain and 52145 isogenic mutant (Benghezal et al., 2006), the isogenic *P. aeruginosa* strains PT5 and PT531 (*rhlR-lasR* avirulent mutant) (Cosson et al., 2002), *E. coli* DH5α (Fisher Scientific), *E. coli* B/r (Gerisch, 1959), non-sporulating *B. subtilis* 36.1 (Ratner and Newell, 1978), and *M. luteus* (Wilczynska and Fisher, 1994). An avirulent strain of *K. pneumoniae* was obtained from ATCC (Strain no. 51697).

The *Dictyostelium* development was performed by spreading 10⁷ amoebae on nitrocellulose filters (47 mm Millipore) on top of absorbent discs pre-soaked in KK2 (0.1 M potassium phosphate pH 6.1) and images were taken at 20 hours [94].

Gene disruption and molecular biology

PIKfyve⁻ cells in an Ax2 background were generated by gene disruption using homologous recombination. A blasticidin knockout cassette was made by amplifying a 5' flanking sequence of the *PIKfyve* gene (DDB_G0279149) (primers: fw- GGTAGATGTTTAGGTGGTGAAGT, rv- gatagctctgcactactgaagCGAGTGGTGGGAATTCATAAAGG) and 3' flanking sequence (primers: fw- ctactggagatccaagctgCCATTCAAGATAGACCAACCAATAG, rv- AGAATCAGAA-TAAACATCACCACC). These primers contained cross over sequences (in lower case) allowing a LoxP-flanked blasticidin resistance cassette (from pDM1079, a kind gift from Douwe Veltman) to be inserted between the two arms.

For *PIKfyve* gene disruption in an Ax3 background a knockout cassette was constructed in pBluescript by sequentially cloning fragment I (amplified by TAGTAGGAGCTCGGATCCG GTAGATGTTTAGGTGGTGAAGTTTTACCAAC and TAGTAGTCTAGACGAGTGGTGA AATTCATAAAGGTACGTTTCAT) and fragment II (amplified by TAGTAGAAGCTTCCAT TCAAGATAGACCAACCAATAGTAGTCCTGC and TAGTAGGGTACCGGATCCAGT GTGTAAATGAGAATCAGAATAAACATCACC). The blasticidin resistance gene was inserted between fragment I and II as an XbaI–HindIII fragment derived from pBSRδBam [95]. Both constructs were linearised, electroporated into cells and colonies were screened by

PCR. Genomic DNA was extracted from lysing 1×10^6 cells in 100 μ l lysis buffer (10mM Tris-HCl pH8.0, 50 mM KCl, 2.5mM MgCl₂, 0.45% NP40, 0.45% Tween 20) and addition of 2ul of 20mg/ml Proteinase K (NEB) for 5 minutes incubation at room temperature. Proteinase K was inactivated at 95°C for 10 minutes prior to PCR analysis. RT-PCR analysis was performed as previously described [96]. Briefly, total RNA was extracted from 1×10^7 cells using the Roche High Pure total RNA isolation kit. The Thermo RevertAid first strand synthesis kit was then used to synthesise cDNA from 2 μ g RNA using random hexamer primers, and used as template for PCR analysis of transcription. Primers used for gDNA and cDNA PCR screens are listed in S1 Table. After validation, the Ax2-derived PIKfyve mutant strain was designated JSK01, and the two independent Ax3-derived mutants JSK05 and 06.

GFP-2xFYVE was expressed using pJSK489 [41] and GFP-PH_{CRAC} with pDM631 [97]. VatM and VatB were cloned previously [98] but subcloned into the GFP-fusion expression vectors pDM352 and 353 [99] to give plasmids pMJC25 and pMJC31 respectively.

Microscopy and image analysis

Fluorescence microscopy was performed on a Perkin-Elmer Ultraview VoX spinning disk confocal microscope running on an Olympus 1x81 body with an UplanSApo 60x oil immersion objective (NA 1.4). Images were captured on a Hamamatsu C9100-50 EM-CCD camera using Volocity software by illuminating cells with 488 nm and 594 nm laser lines. Quantification was performed using Image J (<https://imagej.nih.gov>).

To image PI(3)P dynamics, cells were incubated in HL5 medium at 4°C for 5 mins before addition of 10 μ l of washed 3 μ m latex beads (Sigma LB30) and centrifugation at 280 x g for 10 seconds in glass-bottomed dishes (Mat-Tek). Dishes were removed from ice and incubated at room temperature for 5 mins before imaging. Images were taken every 30 s across 3 fields of view for up to 30 mins.

V-ATPase recruitment and acidification was performed using *Saccharomyces cerevisiae* labelled with pHrodo red (Life Technologies) as per the manufacturers instructions. *Dictyostelium* cells in HL5 medium were incubated with 1×10^7 yeast per 3 cm dish, and allowed to settle for 10 mins before the medium was removed and cells were gently compressed under a 1% agarose/HL5 disk. Images were taken every 10 s across 3 fields of view for up to 20 mins. Yeast particles were identified using the “analyse particles” plugin and mean fluorescence measured over time. V-ATPase recruitment was measured as the mean fluorescence within a 0.5 μ m wide ring selection around the yeast. The signal was then normalised to the initial fluorescence after yeast internalisation for each cell.

Endocytosis and exocytosis

To measure endocytosis, *Dictyostelium* at 5×10^6 cells/ml were shaken at 180 rpm for 15 mins in HL5 before addition of FITC dextran to a final concentration of 2 mg/ml (molecular mass, 70 kDa; Sigma). At each time point 500 μ l of cell suspension were added to 1 ml ice-cold KK2 on ice. Cells were pelleted at 800 x g for 2 mins and washed once in KK2. The pellet was lysed in 50 mM Na₂HPO₄ pH 9.3 0.2% Triton X-100 and measured in a fluorimeter. To measure exocytosis, cells were prepared as above and incubated in 2 mg/ml FITC-dextran overnight. Cells were pelleted, washed twice in HL5 and resuspended in HL5 at 5×10^6 cells/ml. 500 μ l of cell suspension were taken for each time point and treated as described above.

Phagocytosis and phagosomal activity assays

Phagocytosis of *E. coli* was monitored by the decrease in turbidity of the bacterial suspension over time as described [100]. An equal volume of 2×10^7 *Dictyostelium* cells was added to a

bacterial suspension with an $OD_{600\text{ nm}}$ of 0.8, shaking at 180 rpm, and the decrease in $OD_{600\text{ nm}}$ was recorded over time. Phagocytosis of GFP-expressing *M. smegmatis* and 1 μm YG-carboxylated polystyrene beads (Polysciences Inc.) was previously described [55, 101]. 2×10^6 *Dictyostelium*/ml were shaken for 2 hours at 150 rpm. Either 1 μm beads (at a ratio of 200:1) or *M. smegmatis* (multiplicity of infection (MOI) 100) were added, 500 μl aliquots of cells were taken at each time point and fluorescence was measured by flow cytometry [55].

Phagosomal pH and proteolytic activity were measured by feeding cells either FITC/TRITC or DQgreen- BSA/Alexa 594-labelled 3 μm silica beads (Kisker Biotech) [55]. Briefly, cells were seeded in a 96 well plate before addition of beads and fluorescence measured on a plate reader over time. pH values were determined by the ratio of FITC to TRITC fluorescence using a calibration curve and relative proteolysis was normalised to Alexa594 fluorescence. To measure proteolytic activity in cell lysates 4×10^7 cells/ml were resuspended in 150 mM potassium acetate pH 4.0 and lysed by 3 cycles of freeze/thaw in liquid nitrogen. After pelleting cell debris at $18,000 \times g$ for 5 minutes at 4°C , 100 μl of lysate was added per well. Proteolytic activity was measured on a plate reader in triplicate, as described above, using 1×10^8 DQ-BSA/Alexa594 beads per cell. A 5 \times final concentration of HALT protease inhibitor cocktail (Life Technologies) was added to samples as a negative control.

Phagosome isolation and blotting

Dictyostelium phagosomes were purified at different stages in maturation after engulfment of latex beads as previously described [102]. Briefly 10^9 cells per timepoint were incubated with a 200-fold excess of 0.8 μm diameter beads (Sigma) first in 5 ml ice-cold Soerensen buffer containing 120 mM sorbitol (SSB) pH 8 for 5 minutes, then added to 100 ml room-temperature HL5 medium in shaking culture (120 rpm) for 5 (first time point) or 15 minutes to allow phagocytosis (pulse). Engulfment was stopped by adding cells to 300ml ice-cold SSB and centrifugation. After washing away non-engulfed beads, cells were again shaken in room-temperature HL5 for the times indicated (chase) to allow maturation. At each time point, maturation was stopped using ice-cold SSB as above, and cells pelleted. Phagosomes were purified as in [58], after homogenization using 10-passages through a ball homogeniser (void clearance 10 μm). The homogenate was incubated with 10 mM Mg-ATP (Sigma) for 15 minutes before loading onto a discontinuous sucrose gradient. Phagosomes were collected from the 10–25% interface, normalised by light scattering at 600 nm and analysed by Western blot. Antibodies used were anti-VatA mAb 221-35-2 (gift from G. Gerisch), anti-VatM mAb N2 [103]; rabbit anti-cathepsin D [104] and anti-Abp1 [105]. All blots were processed in parallel from the same lysates with identical exposure and processing between cell lines.

Bacteria killing assay

Killing of GFP-expressing *K. pneumoniae* was measured as previously described [61]. Briefly, 10 μl of an overnight culture of bacteria in 280 μl HL5 was placed in a glass-bottomed dish and allowed to settle before careful addition of 1.5 ml of a *Dictyostelium* cell suspension at 1×10^6 cells/ml. Images were taken every 20 s for 40 min at 20 \times magnification. Survival time was determined by how long the GFP-fluorescence persisted after phagocytosis.

Western blotting

Ax2 or *PIKfyve*⁻ cells expressing GFP-VatM or VatB-GFP were analysed by SDS-PAGE and Western blot using a rabbit anti-GFP primary antibody (gift from A. Peden) and a fluorescently conjugated anti-rabbit 800 secondary antibody, using standard techniques. The

endogenous biotinylated mitochondrial protein Methylcrotonoyl-CoA Carboxylase 1 (MCCC1) was used as a loading control using Alexa680-conjugated Streptavidin (Life Technologies) [106].

Legionella infection assays

The following *L. pneumophila* Philadelphia-1 strains were used: virulent JR32 [107], the isogenic $\Delta icmT$ deletion mutant GS3011 lacking a functional Icm/Dot type IV secretion system [74], and corresponding strains constitutively producing GFP [75]. *L. pneumophila* was grown for 3 days on charcoal yeast extract (CYE) agar plates, buffered with *N*-(2-acetamido)-2-aminoethane-sulfonic acid (ACES) [108]. For infections, liquid cultures were inoculated in AYE medium at an OD₆₀₀ of 0.1 and grown for 21 h at 37°C (post-exponential growth phase). To maintain plasmids, chloramphenicol was added at 5 µg/ml.

Uptake by *D. discoideum*, intracellular replication or killing of GFP-producing *L. pneumophila* was analyzed by flow cytometry as described [72]. Exponentially growing amoebae were seeded onto a 24-well plate (1×10^6 cells/ml HL5 medium per well) and allowed to adhere for at least 1–2 h. *L. pneumophila* grown for 21 h in AYE medium was diluted in HL5 medium and used to infect the amoebae at an MOI of 50. The infection was synchronised by centrifugation (10 min, 500 x g), and infected cells were incubated at 25°C for 30 min before extracellular bacteria were removed by washing twice with SorC (2 mM Na₂HPO₄, 15 mM KH₂PO₄, 50 µM CaCl₂, pH 6.0). Infected amoebae were detached by vigorously pipetting and fixed (PFA 2%, sucrose 125 mM, picric acid 15%, in PIPES buffer, pH 6.0), and 1×10^4 amoebae per sample were analyzed using a LSR II Fortessa analyser. The GFP fluorescence intensity falling into a *Dictyostelium* scatter gate was quantified using FlowJo software (Treestar, <http://www.treestar.com>).

Alternatively, intracellular replication of *L. pneumophila* in *D. discoideum* was quantified by determining colony forming units (CFU) in the supernatant as described [72, 109]. Exponentially growing amoebae were washed and resuspended in MB medium (7 g of yeast extract, 14 g of thiotone E peptone, 20 mM MES in 1 l of H₂O, pH 6.9). Amoebae (1×10^5 cells per well) were seeded onto a 96-well plate, allowed to adhere for at least 2 h, and infected at an MOI of 0.1 with *L. pneumophila* grown in AYE medium for 21 h and diluted in MB medium. The infection was synchronised by centrifugation, and the infected amoebae were incubated at 25°C. At the time points indicated, the number of bacteria released into the supernatant was quantified by plating aliquots (10–20 µl) of appropriate dilutions on CYE plates. Intracellular bacteria were also quantified by counting CFU after lysis of the infected amoebae with saponin. At the time points indicated host cells were detached by vigorous pipetting and lysed by incubation with saponin (final concentration– 0.8%) for 10 min. The number of bacteria released into the supernatant was quantified by plating 20 µl aliquots of appropriate dilutions on CYE plates.

Statistics

Statistical analysis was performed using Graphpad Prism 7 software. Biological replicate numbers and statistical tests used for each experiment are detailed in each figure legend. A p-value of <0.05 were deemed significant with * indicating p<0.05, **p<0.01 and ***p<0.005 throughout.

Supporting information

S1 Fig. PIKfyve gene disruption. (A) Schematic representation of the *Dictyostelium* PIKfyve genomic locus indicating the homology arms, blasticidin resistance cassette. Primers used to screen the mutated locus are shown and labelled as circled numbers. (B) PCR screens of the genomic locus for strains JSK06 (Ax3-derived *PIKfyve*- (1)) and the Ax2-derived mutant

JSK01. Three primer combinations were used to verify correct recombination, and loss of the wild-type allele. (C) Confirmation of loss of PIKfyve mRNA by RT-PCR. The mitochondrial large subunit rRNA Ig7 was used as positive control, as well as primers to the gene either 5' or 3' to the blasticidin insertion site. Primer sequences used are listed in [S1 Table](#).
(TIF)

S2 Fig. PIKfyve is not required for development. (A) Images of *Dictyostelium* fruiting bodies formed on filter discs, indicating a normal morphology and proportioning in the absence of PIKfyve. (B) Higher magnification differential interference contrast (DIC) images of pores collected from the fruiting bodies in (A).
(TIF)

S3 Fig. Conservation of PIKfyve-null phenotypes in Ax2-derived mutants. Phagocytosis of (A) of 1 μm beads or (B) GFP-expressing *Mycobacterium smegmatis* measured by flow cytometry, is normal in PIKfyve-null cells. (C) Growth on lawns of *K. pneumoniae* is impaired. Colony diameter over time is plotted in (D). All data are means \pm SD.
(TIF)

S4 Fig. Acidification of macropinosomes in PIKfyve-null cells. Cells were incubated in a mixture of 0.4 mg/ml FITC and 4 mg/ml TRITC dextran for the times indicated. Images were then captured on a confocal microscope. In this assay, vesicles of a neutral pH are yellow and become progressively more red as they acidify and FITC fluorescence is quenched. PIKfyve-cells remain able to acidify their macropinosomes within 10 minutes.
(TIF)

S5 Fig. VatB-GFP expression has a dominant negative effect on acidification. (A) Western blot of cells expressing VatB-GFP or GFP-VatM, probed with an anti-GFP antibody (green). There was no difference in expression levels between Ax2 and PIKfyve⁻ cells for either reporter. However, VatB-GFP was expressed at higher levels than GFP-VatM, likely because it is present in 3 copies per V-ATPase complex. Loading control is the mitochondrial protein MCCC1, recognised by Alexa680-conjugated streptavidin (red). (B) Recruitment of VatB-GFP to phagosomes containing pHrodo-labelled yeast. (C) Automated image analysis of VatB-GFP recruitment as described in [Fig 3](#), showing reduced recruitment in PIKfyve-null cells. (D) Phagosome acidification, measured by the increase in pHrodo fluorescence over time. Note that expression of VatB-GFP in Ax2 cells significantly reduces phagosome acidification relative to GFP-VatM expressing cells, indicating disruption of V-ATPase activity. Values plotted are mean \pm SEM.
(TIF)

S6 Fig. Apilimod recapitulates PIKfyve knockout phenotypes. (A) Phagosomal proteolysis of Ax2 cells either untreated, or treated with 5 μM apilimod. As defects are in hydrolase delivery rather than activity, cells were pre-treated for 2 hours prior to the experiment. (B) Intracellular survival of GFP-expressing *Klebsiella pneumoniae* determined by the time taken for GFP fluorescence to be quenched post-phagocytosis.
(TIF)

S1 Table. Primers used for screening and validating PIKfyve gene disruption.
(DOCX)

Acknowledgments

The authors would like to thank Phill Hawkins and his group for their endeavours to separate *Dictyostelium* PIP₂s.

Author Contributions

Conceptualization: Catherine M. Buckley, Victoria L. Heath, Stephen K. Dove, Robert H. Michell, Hubert Hilbi, Thierry Soldati, Robert H. Insall, Jason S. King.

Formal analysis: Catherine M. Buckley, Jason S. King.

Funding acquisition: Stephen K. Dove, Hubert Hilbi, Robert H. Insall, Jason S. King.

Investigation: Catherine M. Buckley, Victoria L. Heath, Aurélie Guého, Cristina Bosmani, Paulina Knobloch, Phumzile Sikakana, Nicolas Personnic, Roger Meier, Jason S. King.

Methodology: Catherine M. Buckley, Victoria L. Heath, Aurélie Guého, Cristina Bosmani, Paulina Knobloch, Nicolas Personnic, Roger Meier, Hubert Hilbi, Thierry Soldati, Robert H. Insall, Jason S. King.

Project administration: Stephen K. Dove, Thierry Soldati, Jason S. King.

Resources: Thierry Soldati, Robert H. Insall, Jason S. King.

Supervision: Stephen K. Dove, Hubert Hilbi, Thierry Soldati, Robert H. Insall, Jason S. King.

Validation: Jason S. King.

Writing – original draft: Catherine M. Buckley, Jason S. King.

Writing – review & editing: Catherine M. Buckley, Victoria L. Heath, Cristina Bosmani, Paulina Knobloch, Nicolas Personnic, Robert H. Michell, Hubert Hilbi, Thierry Soldati, Robert H. Insall, Jason S. King.

References

1. Flannagan RS, Cosio G, Grinstein S. Antimicrobial mechanisms of phagocytes and bacterial evasion strategies. *Nat Rev Microbiol*. 2009; 7(5):355–66. Epub 2009/04/17. <https://doi.org/10.1038/nrmicro2128> PMID: [19369951](https://pubmed.ncbi.nlm.nih.gov/19369951/).
2. Di Paolo G, De Camilli P. Phosphoinositides in cell regulation and membrane dynamics. *Nature*. 2006; 443(7112):651–7. <https://doi.org/10.1038/nature05185> PMID: [17035995](https://pubmed.ncbi.nlm.nih.gov/17035995/).
3. Levin R, Grinstein S, Schlam D. Phosphoinositides in phagocytosis and macropinocytosis. *Biochim Biophys Acta*. 2015; 1851(6):805–23. <https://doi.org/10.1016/j.bbailip.2014.09.005> PMID: [25238964](https://pubmed.ncbi.nlm.nih.gov/25238964/).
4. Gaullier JM, Simonsen A, D'Arrigo A, Bremnes B, Stenmark H, Aasland R. FYVE fingers bind PtdIns (3)P. *Nature*. 1998; 394(6692):432–3. <https://doi.org/10.1038/28767> PMID: [9697764](https://pubmed.ncbi.nlm.nih.gov/9697764/).
5. Raiborg C, Bremnes B, Mehlum A, Gillooly DJ, D'Arrigo A, Stang E, et al. FYVE and coiled-coil domains determine the specific localisation of Hrs to early endosomes. *J Cell Sci*. 2001; 114(Pt 12):2255–63. PMID: [11493665](https://pubmed.ncbi.nlm.nih.gov/11493665/).
6. Cabezas A, Pattni K, Stenmark H. Cloning and subcellular localization of a human phosphatidylinositol 3-phosphate 5-kinase, PIKfyve/Fab1. *Gene*. 2006; 371(1):34–41. <https://doi.org/10.1016/j.gene.2005.11.009> PMID: [16448788](https://pubmed.ncbi.nlm.nih.gov/16448788/).
7. Michell RH, Heath VL, Lemmon MA, Dove SK. Phosphatidylinositol 3,5-bisphosphate: metabolism and cellular functions. *Trends Biochem Sci*. 2006; 31(1):52–63. <https://doi.org/10.1016/j.tibs.2005.11.013> PMID: [16364647](https://pubmed.ncbi.nlm.nih.gov/16364647/).
8. Sbrissa D, Ikononov OC, Shisheva A. PIKfyve, a mammalian ortholog of yeast Fab1p lipid kinase, synthesizes 5-phosphoinositides. Effect of insulin. *J Biol Chem*. 1999; 274(31):21589–97. PMID: [10419465](https://pubmed.ncbi.nlm.nih.gov/10419465/).
9. Zolov SN, Bridges D, Zhang Y, Lee WW, Riehle E, Verma R, et al. In vivo, Pikfyve generates PI(3,5)P₂, which serves as both a signaling lipid and the major precursor for PI5P. *Proc Natl Acad Sci U S A*. 2012; 109(43):17472–7. <https://doi.org/10.1073/pnas.1203106109> PMID: [23047693](https://pubmed.ncbi.nlm.nih.gov/23047693/); PubMed Central PMCID: PMC3491506.
10. Yamamoto A, DeWald DB, Boronenkov IV, Anderson RA, Emr SD, Koshland D. Novel PI(4)P 5-kinase homologue, Fab1p, essential for normal vacuole function and morphology in yeast. *Mol Biol Cell*. 1995; 6(5):525–39. PMID: [7663021](https://pubmed.ncbi.nlm.nih.gov/7663021/); PubMed Central PMCID: PMC301213.

11. Takasuga S, Sasaki T. Phosphatidylinositol-3,5-bisphosphate: metabolism and physiological functions. *J Biochem*. 2013; 154(3):211–8. <https://doi.org/10.1093/jb/mvt064> PMID: [23857703](#).
12. McCartney AJ, Zhang Y, Weisman LS. Phosphatidylinositol 3,5-bisphosphate: low abundance, high significance. *BioEssays: news and reviews in molecular, cellular and developmental biology*. 2014; 36(1):52–64. <https://doi.org/10.1002/bies.201300012> PMID: [24323921](#); PubMed Central PMCID: [PMCPMC3906640](#).
13. Ho CY, Alghamdi TA, Botelho RJ. Phosphatidylinositol-3,5-bisphosphate: no longer the poor PIP2. *Traffic*. 2012; 13(1):1–8. <https://doi.org/10.1111/j.1600-0854.2011.01246.x> PMID: [21736686](#).
14. Michell RH. Inositol lipids: from an archaeal origin to phosphatidylinositol 3,5-bisphosphate faults in human disease. *FEBS J*. 2013; 280(24):6281–94. <https://doi.org/10.1111/febs.12452> PMID: [23902363](#).
15. Ikononov O, Sbrissa D, Shisheva A. Mammalian cell morphology and endocytic membrane homeostasis require enzymatically active phosphoinositide 5-kinase PIKfyve. *J Biol Chem*. 2001; 276(28):26141–7. <https://doi.org/10.1074/jbc.M101722200> PMID: [11285266](#).
16. Ikononov OC, Sbrissa D, Mlak K, Deeb R, Fligger J, Soans A, et al. Active PIKfyve associates with and promotes the membrane attachment of the late endosome-to-trans-Golgi network transport factor Rab9 effector p40. *J Biol Chem*. 2003; 278(51):50863–71. <https://doi.org/10.1074/jbc.M307260200> PMID: [14530284](#).
17. Rutherford AC, Traer C, Wassmer T, Pattni K, Bujny MV, Carlton JG, et al. The mammalian phosphatidylinositol 3-phosphate 5-kinase (PIKfyve) regulates endosome-to-TGN retrograde transport. *J Cell Sci*. 2006; 119(Pt 19):3944–57. <https://doi.org/10.1242/jcs.03153> PMID: [16954148](#); PubMed Central PMCID: [PMC1904490](#).
18. de Lartigue J, Poison H, Feldman M, Shokat K, Tooze SA, Urbán S, et al. PIKfyve Regulation of Endosome-Linked Pathways. *Traffic*. 2009; 10(7):883–93. <https://doi.org/10.1111/j.1600-0854.2009.00915.x> PMID: [19582903](#)
19. Martin S, Harper CB, May LM, Coulson EJ, Meunier FA, Osborne SL. Inhibition of PIKfyve by YM-201636 dysregulates autophagy and leads to apoptosis-independent neuronal cell death. *PLoS One*. 2013; 8(3):e60152. <https://doi.org/10.1371/journal.pone.0060152> PMID: [23544129](#); PubMed Central PMCID: [PMC3609765](#).
20. Rusten T, Vaccari T, Lindmo K, Rodahl L, Nezis I, Sem-Jacobsen C, et al. ESCRTs and Fab1 regulate distinct steps of autophagy. *Curr Biol*. 2007; 17(20):1817–25. <https://doi.org/10.1016/j.cub.2007.09.032> PMID: [17935992](#).
21. Tsuruta F, Green EM, Rousset M, Dolmetsch RE. PIKfyve regulates CaV1.2 degradation and prevents excitotoxic cell death. *J Cell Biol*. 2009; 187(2):279–94. <https://doi.org/10.1083/jcb.200903028> PMID: [19841139](#); PubMed Central PMCID: [PMC2768838](#).
22. Min SH, Suzuki A, Stalker TJ, Zhao L, Wang Y, McKennan C, et al. Loss of PIKfyve in platelets causes a lysosomal disease leading to inflammation and thrombosis in mice. *Nat Commun*. 2014; 5:4691. <https://doi.org/10.1038/ncomms5691> PMID: [25178411](#); PubMed Central PMCID: [PMCPMC4369914](#).
23. Zhang X, Chow CY, Sahenk Z, Shy ME, Meisler MH, Li J. Mutation of FIG4 causes a rapidly progressive, asymmetric neuronal degeneration. *Brain: a journal of neurology*. 2008; 131(Pt 8):1990–2001. <https://doi.org/10.1093/brain/awn114> PMID: [18556664](#); PubMed Central PMCID: [PMC2724900](#).
24. Zhang Y, McCartney AJ, Zolov SN, Ferguson CJ, Meisler MH, Sutton MA, et al. Modulation of synaptic function by VAC14, a protein that regulates the phosphoinositides PI(3,5)P(2) and PI(5)P. *EMBO J*. 2012; 31(16):3442–56. <https://doi.org/10.1038/emboj.2012.200> PMID: [22842785](#); PubMed Central PMCID: [PMC3419932](#).
25. Zhang Y, Zolov SN, Chow CY, Slutsky SG, Richardson SC, Piper RC, et al. Loss of Vac14, a regulator of the signaling lipid phosphatidylinositol 3,5-bisphosphate, results in neurodegeneration in mice. *Proc Natl Acad Sci U S A*. 2007; 104(44):17518–23. <https://doi.org/10.1073/pnas.0702275104> PMID: [17956977](#); PubMed Central PMCID: [PMC2077288](#).
26. Bohdanowicz M, Grinstein S. Role of phospholipids in endocytosis, phagocytosis, and macropinocytosis. *Physiological reviews*. 2013; 93(1):69–106. <https://doi.org/10.1152/physrev.00002.2012> PMID: [23303906](#).
27. Ellison CD, Anderson KE, Morgan G, Chilvers ER, Lipp P, Stephens LR, et al. Phosphatidylinositol 3-phosphate is generated in phagosomal membranes. *Curr Biol*. 2001; 11(20):1631–5. PMID: [11676926](#).
28. Vieira OV, Botelho RJ, Rameh L, Brachmann SM, Matsuo T, Davidson HW, et al. Distinct roles of class I and class III phosphatidylinositol 3-kinases in phagosome formation and maturation. *J Cell Biol*. 2001; 155(1):19–25. <https://doi.org/10.1083/jcb.200107069> PMID: [11581283](#); PubMed Central PMCID: [PMCPMC2150784](#).

29. Fratti RA, Backer JM, Gruenberg J, Corvera S, Deretic V. Role of phosphatidylinositol 3-kinase and Rab5 effectors in phagosomal biogenesis and mycobacterial phagosome maturation arrest. *J Cell Biol.* 2001; 154(3):631–44. <https://doi.org/10.1083/jcb.200106049> PMID: [11489920](https://pubmed.ncbi.nlm.nih.gov/11489920/); PubMed Central PMCID: PMC2196432.
30. Cai X, Xu Y, Cheung AK, Tomlinson RC, Alcazar-Roman A, Murphy L, et al. PIKfyve, a class III PI kinase, is the target of the small molecular IL-12/IL-23 inhibitor apilimod and a player in Toll-like receptor signaling. *Chem Biol.* 2013; 20(7):912–21. <https://doi.org/10.1016/j.chembiol.2013.05.010> PMID: [23890009](https://pubmed.ncbi.nlm.nih.gov/23890009/).
31. Ikononov OC, Sbrissa D, Shisheva A. YM201636, an inhibitor of retroviral budding and PIKfyve-catalyzed PtdIns(3,5)P₂ synthesis, halts glucose entry by insulin in adipocytes. *Biochem Biophys Res Commun.* 2009; 382(3):566–70. <https://doi.org/10.1016/j.bbrc.2009.03.063> PMID: [19289105](https://pubmed.ncbi.nlm.nih.gov/19289105/); PubMed Central PMCID: PMC3910513.
32. Hazeki K, Nigorikawa K, Takaba Y, Segawa T, Nukuda A, Masuda A, et al. Essential roles of PIKfyve and PTEN on phagosomal phosphatidylinositol 3-phosphate dynamics. *FEBS Lett.* 2012; 586(22):4010–5. <https://doi.org/10.1016/j.febslet.2012.09.043> PMID: [23068606](https://pubmed.ncbi.nlm.nih.gov/23068606/).
33. Kim GH, Dayam RM, Prashar A, Terebiznik M, Botelho RJ. PIKfyve Inhibition Interferes with Phagosome and Endosome Maturation in Macrophages. *Traffic.* 2014; 15(10):1143–63. <https://doi.org/10.1111/tra.12199> PMID: [25041080](https://pubmed.ncbi.nlm.nih.gov/25041080/).
34. Choy CH, Saffi G, Gray MA, Wallace C, Dayam RM, Ou ZA, et al. Lysosome enlargement during inhibition of the lipid kinase PIKfyve proceeds through lysosome coalescence. *J Cell Sci.* 2018; 131(10). Epub 2018/04/18. <https://doi.org/10.1242/jcs.213587> PMID: [29661845](https://pubmed.ncbi.nlm.nih.gov/29661845/).
35. Dayam RM, Sun CX, Choy CH, Mancuso G, Glogauer M, Botelho RJ. The Lipid Kinase PIKfyve Coordinates the Neutrophil Immune Response through the Activation of the Rac GTPase. *Journal of immunology.* 2017; 199(6):2096–105. Epub 2017/08/06. <https://doi.org/10.4049/jimmunol.1601466> PMID: [28779020](https://pubmed.ncbi.nlm.nih.gov/28779020/).
36. Nicot AS, Fares H, Payrastré B, Chisholm AD, Labouesse M, Laporte J. The phosphoinositide kinase PIKfyve/Fab1p regulates terminal lysosome maturation in *Caenorhabditis elegans*. *Mol Biol Cell.* 2006; 17(7):3062–74. <https://doi.org/10.1091/mbc.E05-12-1120> PMID: [16801682](https://pubmed.ncbi.nlm.nih.gov/16801682/); PubMed Central PMCID: PMC21483040.
37. Jefferies HB, Cooke FT, Jat P, Boucheron C, Koizumi T, Hayakawa M, et al. A selective PIKfyve inhibitor blocks PtdIns(3,5)P₂ production and disrupts endomembrane transport and retroviral budding. *EMBO reports.* 2008; 9(2):164–70. <https://doi.org/10.1038/sj.embor.7401155> PMID: [18188180](https://pubmed.ncbi.nlm.nih.gov/18188180/); PubMed Central PMCID: PMC2246419.
38. Krishna S, Palm W, Lee Y, Yang W, Bandyopadhyay U, Xu H, et al. PIKfyve Regulates Vacuole Maturation and Nutrient Recovery following Engulfment. *Dev Cell.* 2016; 38(5):536–47. <https://doi.org/10.1016/j.devcel.2016.08.001> PMID: [27623384](https://pubmed.ncbi.nlm.nih.gov/27623384/); PubMed Central PMCID: PMC25046836.
39. Ho CY, Choy CH, Wattson CA, Johnson DE, Botelho RJ. The Fab1/PIKfyve Phosphoinositide Phosphate Kinase Is Not Necessary to Maintain the pH of Lysosomes and of the Yeast Vacuole. *J Biol Chem.* 2015; 290(15):9919–28. <https://doi.org/10.1074/jbc.M114.613984> PMID: [25713145](https://pubmed.ncbi.nlm.nih.gov/25713145/).
40. Clark J, Kay RR, Kielkowska A, Niewczas I, Fets L, Oxley D, et al. Dictyostelium uses ether-linked inositol phospholipids for intracellular signalling. *EMBO J.* 2014; 33(19):2188–200. <https://doi.org/10.15252/embj.201488677> PMID: [25180230](https://pubmed.ncbi.nlm.nih.gov/25180230/); PubMed Central PMCID: PMC24282506.
41. Calvo-Garrido J, King JS, Muñoz-Braceras S, Escalante R. Vmp1 regulates PtdIns3P signaling during autophagosome formation in *Dictyostelium discoideum*. *Traffic.* 2014; 15(11):1235–46. <https://doi.org/10.1111/tra.12210> PMID: [25131297](https://pubmed.ncbi.nlm.nih.gov/25131297/).
42. King JS, Teo R, Ryves J, Reddy JV, Peters O, Orabi B, et al. The mood stabiliser lithium suppresses PIP3 signalling in *Dictyostelium* and human cells. *Dis Model Mech.* 2009; 2(5–6):306–12. <https://doi.org/10.1242/dmm.001271> PMID: [19383941](https://pubmed.ncbi.nlm.nih.gov/19383941/); PubMed Central PMCID: PMC2675811.
43. Kortholt A, King JS, Keizer-Gunnink I, Harwood AJ, Van Haastert PJ. Phospholipase C regulation of phosphatidylinositol 3,4,5-trisphosphate-mediated chemotaxis. *Mol Biol Cell.* 2007; 18(12):4772–9. <https://doi.org/10.1091/mbc.E07-05-0407> PMID: [17898079](https://pubmed.ncbi.nlm.nih.gov/17898079/); PubMed Central PMCID: PMC2096598.
44. Dormann D, Weijer G, Dowler S, Weijer CJ. In vivo analysis of 3-phosphoinositide dynamics during *Dictyostelium* phagocytosis and chemotaxis. *J Cell Sci.* 2004; 117(Pt 26):6497–509. <https://doi.org/10.1242/jcs.01579> PMID: [15572406](https://pubmed.ncbi.nlm.nih.gov/15572406/).
45. Nicot AS, Fares H, Payrastré B, Chisholm AD, Labouesse M, Laporte J. The phosphoinositide kinase PIKfyve/Fab1p regulates terminal lysosome maturation in *Caenorhabditis elegans*. *Molecular biology of the cell.* 2006; 17(7):3062–74. PubMed PMID: WOS:000238721000018. <https://doi.org/10.1091/mbc.E05-12-1120> PMID: [16801682](https://pubmed.ncbi.nlm.nih.gov/16801682/)

46. Clarke M, Maddera L, Engel U, Gerisch G. Retrieval of the vacuolar H-ATPase from phagosomes revealed by live cell imaging. *PLoS One*. 2010; 5(1):e8585. <https://doi.org/10.1371/journal.pone.0008585> PMID: [20052281](https://pubmed.ncbi.nlm.nih.gov/20052281/); PubMed Central PMCID: PMCPMC2796722.
47. Smith EW, Lima WC, Charette SJ, Cosson P. Effect of starvation on the endocytic pathway in Dictyostelium cells. *Eukaryot Cell*. 2010; 9(3):387–92. <https://doi.org/10.1128/EC.00285-09> PMID: [20097741](https://pubmed.ncbi.nlm.nih.gov/20097741/); PubMed Central PMCID: PMCPMC2837978.
48. Veltman DM, Williams TD, Bloomfield G, Chen BC, Betzig E, Insall RH, et al. A plasma membrane template for macropinosomes. *eLife*. 2016; 5. <https://doi.org/10.7554/eLife.20085> PMID: [27960076](https://pubmed.ncbi.nlm.nih.gov/27960076/); PubMed Central PMCID: PMCPMC5154761.
49. Williams TD, Kay RR. The physiological regulation of macropinosomes during Dictyostelium growth and development. *J Cell Sci*. 2018; 131(6). Epub 2018/02/15. <https://doi.org/10.1242/jcs.213736> PMID: [29440238](https://pubmed.ncbi.nlm.nih.gov/29440238/); PubMed Central PMCID: PMCPMC5897714.
50. Clarke M, Kohler J, Arana Q, Liu T, Heuser J, Gerisch G. Dynamics of the vacuolar H(+)-ATPase in the contractile vacuole complex and the endosomal pathway of Dictyostelium cells. *J Cell Sci*. 2002; 115(Pt 14):2893–905. PMID: [12082150](https://pubmed.ncbi.nlm.nih.gov/12082150/).
51. Buckley CM, Gopaldass N, Bosmani C, Johnston SA, Soldati T, Insall RH, et al. WASH drives early recycling from macropinosomes and phagosomes to maintain surface phagocytic receptors. *Proc Natl Acad Sci U S A*. 2016; 113(40):E5906–E15. <https://doi.org/10.1073/pnas.1524532113> PMID: [27647881](https://pubmed.ncbi.nlm.nih.gov/27647881/).
52. Gary JD, Wurmser AE, Bonangelino CJ, Weisman LS, Emr SD. Fab1p is essential for PtdIns(3)P 5-kinase activity and the maintenance of vacuolar size and membrane homeostasis. *J Cell Biol*. 1998; 143(1):65–79. PMID: [9763421](https://pubmed.ncbi.nlm.nih.gov/9763421/); PubMed Central PMCID: PMC2132800.
53. Kerr MC, Wang JT, Castro NA, Hamilton NA, Town L, Brown DL, et al. Inhibition of the PtdIns (5) kinase PIKfyve disrupts intracellular replication of Salmonella. *The EMBO journal*. 2010; 29(8):1331–47. <https://doi.org/10.1038/emboj.2010.28> PMID: [20300065](https://pubmed.ncbi.nlm.nih.gov/20300065/)
54. Bak G, Lee EJ, Lee Y, Kato M, Segami S, Sze H, et al. Rapid structural changes and acidification of guard cell vacuoles during stomatal closure require phosphatidylinositol 3,5-bisphosphate. *Plant Cell*. 2013; 25(6):2202–16. <https://doi.org/10.1105/tpc.113.110411> PMID: [23757398](https://pubmed.ncbi.nlm.nih.gov/23757398/); PubMed Central PMCID: PMC3723621.
55. Sattler N, Monroy R, Soldati T. Quantitative analysis of phagocytosis and phagosome maturation. *Methods in molecular biology*. 2013; 983:383–402. https://doi.org/10.1007/978-1-62703-302-2_21 PMID: [23494319](https://pubmed.ncbi.nlm.nih.gov/23494319/).
56. Li SC, Diakov TT, Xu T, Tarsio M, Zhu W, Couoh-Cardel S, et al. The signaling lipid PI(3,5)P(2) stabilizes V(1)-V(o) sector interactions and activates the V-ATPase. *Mol Biol Cell*. 2014; 25(8):1251–62. <https://doi.org/10.1091/mbc.E13-10-0563> PMID: [24523285](https://pubmed.ncbi.nlm.nih.gov/24523285/); PubMed Central PMCID: PMCPMC3982991.
57. Park L, Thomason PA, Zech T, King JS, Veltman DM, Carnell M, et al. Cyclical action of the WASH complex: FAM21 and capping protein drive WASH recycling, not initial recruitment. *Dev Cell*. 2013; 24(2):169–81. <https://doi.org/10.1016/j.devcel.2012.12.014> PMID: [23369714](https://pubmed.ncbi.nlm.nih.gov/23369714/).
58. Gopaldass N, Patel D, Kratzke R, Dieckmann R, Hausherr S, Hagedorn M, et al. Dynamin A, Myosin IB and Abp1 couple phagosome maturation to F-actin binding. *Traffic*. 2012; 13(1):120–30. <https://doi.org/10.1111/j.1600-0854.2011.01296.x> PMID: [22008230](https://pubmed.ncbi.nlm.nih.gov/22008230/).
59. Simonsen A, Lippe R, Christoforidis S, Gaullier JM, Brech A, Callaghan J, et al. EEA1 links PI(3)K function to Rab5 regulation of endosome fusion. *Nature*. 1998; 394(6692):494–8. <https://doi.org/10.1038/28879> PMID: [9697774](https://pubmed.ncbi.nlm.nih.gov/9697774/).
60. Gillooly DJ, Morrow IC, Lindsay M, Gould R, Bryant NJ, Gaullier JM, et al. Localization of phosphatidylinositol 3-phosphate in yeast and mammalian cells. *Embo Journal*. 2000; 19(17):4577–88. <https://doi.org/10.1093/emboj/19.17.4577> PubMed PMID: WOS:000089275600016. PMID: [10970851](https://pubmed.ncbi.nlm.nih.gov/10970851/)
61. Leiba J, Sabra A, Bodinier R, Marchetti A, Lima WC, Melotti A, et al. Vps13F links bacterial recognition and intracellular killing in Dictyostelium. *Cell Microbiol*. 2017. <https://doi.org/10.1111/cmi.12722> PMID: [28076662](https://pubmed.ncbi.nlm.nih.gov/28076662/).
62. Froquet R, Lelong E, Marchetti A, Cosson P. Dictyostelium discoideum: a model host to measure bacterial virulence. *Nat Protoc*. 2009; 4(1):25–30. <https://doi.org/10.1038/nprot.2008.212> PMID: [19131953](https://pubmed.ncbi.nlm.nih.gov/19131953/).
63. Hilbi H, Hoffmann C, Harrison CF. Legionella spp. outdoors: colonization, communication and persistence. *Environ Microbiol Rep*. 2011; 3(3):286–96. <https://doi.org/10.1111/j.1758-2229.2011.00247.x> PMID: [23761274](https://pubmed.ncbi.nlm.nih.gov/23761274/).
64. Finsel I, Hilbi H. Formation of a pathogen vacuole according to Legionella pneumophila: how to kill one bird with many stones. *Cell Microbiol*. 2015; 17(7):935–50. <https://doi.org/10.1111/cmi.12450> PMID: [25903720](https://pubmed.ncbi.nlm.nih.gov/25903720/).

65. Ge J, Shao F. Manipulation of host vesicular trafficking and innate immune defence by *Legionella* Dot/Icm effectors. *Cell Microbiol.* 2011; 13(12):1870–80. <https://doi.org/10.1111/j.1462-5822.2011.01710.x> PMID: [21981078](#).
66. Weber S, Wagner M, Hilbi H. Live-cell imaging of phosphoinositide dynamics and membrane architecture during *Legionella* infection. *MBio.* 2014; 5(1):e00839–13. <https://doi.org/10.1128/mBio.00839-13> PMID: [24473127](#); PubMed Central PMCID: PMC3903275.
67. Brombacher E, Urwyler S, Ragaz C, Weber SS, Kami K, Overduin M, et al. Rab1 guanine nucleotide exchange factor SidM is a major phosphatidylinositol 4-phosphate-binding effector protein of *Legionella pneumophila*. *J Biol Chem.* 2009; 284(8):4846–56. <https://doi.org/10.1074/jbc.M807505200> PMID: [19095644](#); PubMed Central PMCID: PMC2643517.
68. Hilbi H, Weber S, Finsel I. Anchors for effectors: subversion of phosphoinositide lipids by *Legionella*. *Front Microbiol.* 2011; 2:91. <https://doi.org/10.3389/fmicb.2011.00091> PMID: [21833330](#); PubMed Central PMCID: PMC3153050.
69. Jank T, Bohmer KE, Tzivelekidis T, Schwan C, Belyi Y, Aktories K. Domain organization of *Legionella* effector SetA. *Cell Microbiol.* 2012; 14(6):852–68. <https://doi.org/10.1111/j.1462-5822.2012.01761.x> PMID: [22288428](#).
70. Finsel I, Ragaz C, Hoffmann C, Harrison CF, Weber S, van Rahden VA, et al. The *Legionella* effector RidL inhibits retrograde trafficking to promote intracellular replication. *Cell Host Microbe.* 2013; 14(1):38–50. <https://doi.org/10.1016/j.chom.2013.06.001> PMID: [23870312](#).
71. Harding CR, Mattheis C, Mousnier A, Oates CV, Hartland EL, Frankel G, et al. LtpD Is a Novel *Legionella pneumophila* Effector That Binds Phosphatidylinositol 3-Phosphate and Inositol Monophosphatase IMPA1. *Infection and Immunity.* 2013; 81(11):4261–70. <https://doi.org/10.1128/IAI.01054-13> PubMed PMID: WOS:000325719900031. PMID: [24002062](#)
72. Weber SS, Ragaz C, Reus K, Nyfeler Y, Hilbi H. *Legionella pneumophila* exploits PI(4)P to anchor secreted effector proteins to the replicative vacuole. *Plos Pathogens.* 2006; 2(5):418–30. doi: ARTN e46 <https://doi.org/10.1371/journal.ppat.0020046> PubMed PMID: WOS:000202894500009. PMID: [16710455](#)
73. Dolinsky S, Haneburger I, Cichy A, Hannemann M, Itzen A, Hilbi H. The *Legionella longbeachae* Icm/Dot substrate SidC selectively binds phosphatidylinositol 4-phosphate with nanomolar affinity and promotes pathogen vacuole-endoplasmic reticulum interactions. *Infect Immun.* 2014; 82(10):4021–33. <https://doi.org/10.1128/IAI.01685-14> PMID: [25024371](#); PubMed Central PMCID: PMC3903275.
74. Segal G, Shuman HA. Intracellular multiplication and human macrophage killing by *Legionella pneumophila* are inhibited by conjugal components of IncQ plasmid RSF1010. *Molecular Microbiology.* 1998; 30(1):197–208. <https://doi.org/10.1046/j.1365-2958.1998.01054.x> PubMed PMID: WOS:000076538500017. PMID: [9786196](#)
75. Hilbi H, Segal G, Shuman HA. Icm/dot-dependent upregulation of phagocytosis by *Legionella pneumophila*. *Mol Microbiol.* 2001; 42(3):603–17. PMID: [11722729](#).
76. Rizopoulos Z, Balistreri G, Kilcher S, Martin CK, Syedbasha M, Helenius A, et al. Vaccinia Virus Infection Requires Maturation of Macropinosomes. *Traffic.* 2015; 16(8):814–31. <https://doi.org/10.1111/tra.12290> PMID: [25869659](#); PubMed Central PMCID: PMC3903275.
77. Sbrissa D, Ikononov OC, Shisheva A. PIKfyve lipid kinase is a protein kinase: downregulation of 5'-phosphoinositide product formation by autophosphorylation. *Biochemistry.* 2000; 39(51):15980–9. Epub 2000/12/22. PMID: [11123925](#).
78. Dong XP, Shen D, Wang X, Dawson T, Li X, Zhang Q, et al. PI(3,5)P(2) controls membrane trafficking by direct activation of mucolipin Ca(2+) release channels in the endolysosome. *Nat Commun.* 2010; 1:38. <https://doi.org/10.1038/ncomms1037> PMID: [20802798](#); PubMed Central PMCID: PMC3903275.
79. Dayam RM, Saric A, Shilliday RE, Botelho RJ. The Phosphoinositide-Gated Lysosomal Ca(2+) Channel, TRPML1, Is Required for Phagosome Maturation. *Traffic.* 2015; 16(9):1010–26. <https://doi.org/10.1111/tra.12303> PMID: [26010303](#).
80. Li X, Rydzewski N, Hider A, Zhang X, Yang J, Wang W, et al. A molecular mechanism to regulate lysosome motility for lysosome positioning and tubulation. *Nat Cell Biol.* 2016; 18(4):404–17. <https://doi.org/10.1038/ncb3324> PMID: [26950892](#).
81. Lima WC, Leuba F, Soldati T, Cosson P. Mucolipin controls lysosome exocytosis in *Dictyostelium*. *J Cell Sci.* 2012; 125(Pt 9):2315–22. <https://doi.org/10.1242/jcs.100362> PMID: [22357942](#).
82. Horwitz MA. THE LEGIONNAIRES-DISEASE BACTERIUM (*LEGIONELLA-PNEUMOPHILA*) INHIBITS PHAGOSOME-LYSOSOME FUSION IN HUMAN-MONOCYTES. *Journal of Experimental Medicine.* 1983; 158(6):2108–26. <https://doi.org/10.1084/jem.158.6.2108> PubMed PMID: WOS: A1983RV00200023. PMID: [6644240](#)

83. Lamothe J, Huynh KK, Grinstein S, Valvano MA. Intracellular survival of *Burkholderia cenocepacia* in macrophages is associated with a delay in the maturation of bacteria-containing vacuoles. *Cell Microbiol.* 2007; 9(1):40–53. <https://doi.org/10.1111/j.1462-5822.2006.00766.x> PMID: 16869828.
84. Smith LM, Dixon EF, May RC. The fungal pathogen *Cryptococcus neoformans* manipulates macrophage phagosome maturation. *Cell Microbiol.* 2015; 17(5):702–13. <https://doi.org/10.1111/cmi.12394> PMID: 25394938.
85. Segal G, Shuman HA. *Legionella pneumophila* utilizes the same genes to multiply within *Acanthamoeba castellanii* and human macrophages. *Infection and Immunity.* 1999; 67(5):2117–24. PubMed PMID: WOS:000079909300010. PMID: 10225863
86. Steenbergen JN, Shuman HA, Casadevall A. *Cryptococcus neoformans* interactions with amoebae suggest an explanation for its virulence and intracellular pathogenic strategy in macrophages. *Proc Natl Acad Sci U S A.* 2001; 98(26):15245–50. <https://doi.org/10.1073/pnas.261418798> PMID: 11742090; PubMed Central PMCID: PMC65014.
87. Hasselbring BM, Patel MK, Schell MA. *Dictyostelium discoideum* as a model system for identification of *Burkholderia pseudomallei* virulence factors. *Infect Immun.* 2011; 79(5):2079–88. <https://doi.org/10.1128/IAI.01233-10> PMID: 21402765; PubMed Central PMCID: PMC3088138.
88. Hubber A, Roy CR. Modulation of host cell function by *Legionella pneumophila* type IV effectors. *Annu Rev Cell Dev Biol.* 2010; 26:261–83. <https://doi.org/10.1146/annurev-cellbio-100109-104034> PMID: 20929312.
89. Isberg RR, O'Connor TJ, Heidtman M. The *Legionella pneumophila* replication vacuole: making a cosy niche inside host cells. *Nature Reviews Microbiology.* 2009; 7(1):12–24. <https://doi.org/10.1038/nrmicro1967> PubMed PMID: WOS:000262110300009. PMID: 19011659
90. Zhao J, Beyrakhova K, Liu Y, Alvarez CP, Bueler SA, Xu L, et al. Molecular basis for the binding and modulation of V-ATPase by a bacterial effector protein. *PLoS Pathog.* 2017; 13(6):e1006394. Epub 2017/06/02. <https://doi.org/10.1371/journal.ppat.1006394> PMID: 28570695; PubMed Central PMCID: PMC5469503.
91. Xu L, Shen X, Bryan A, Banga S, Swanson MS, Luo ZQ. Inhibition of host vacuolar H⁺-ATPase activity by a *Legionella pneumophila* effector. *PLoS Pathog.* 2010; 6(3):e1000822. Epub 2010/03/25. <https://doi.org/10.1371/journal.ppat.1000822> PMID: 20333253; PubMed Central PMCID: PMC2841630.
92. Lima WC, Pillonel T, Bertelli C, Ifrid E, Greub G, Cosson P. Genome sequencing and functional characterization of the non-pathogenic *Klebsiella pneumoniae* KpGe bacteria. *Microbes and infection / Institut Pasteur.* 2018; 20(5):293–301. Epub 2018/05/14. <https://doi.org/10.1016/j.micinf.2018.04.001> PMID: 29753816.
93. Froquet R, Lelong E, Marchetti A, Cosson P. *Dictyostelium discoideum*: a model host to measure bacterial virulence. *Nature Protocols.* 2009; 4(1):25–30. <https://doi.org/10.1038/nprot.2008.212> PubMed PMID: WOS:000265781800003. PMID: 19131953
94. Wilkins A, Khosla M, Fraser DJ, Spiegelman GB, Fisher PR, Weeks G, et al. *Dictyostelium RasD* is required for normal phototaxis, but not differentiation. *Genes Dev.* 2000; 14(11):1407–13. PMID: 10837033; PubMed Central PMCID: PMC316659.
95. Sutoh K. A transformation vector for *dictyostelium discoideum* with a new selectable marker bsr. *Plasmid.* 1993; 30(2):150–4. <https://doi.org/10.1006/plas.1993.1042> PMID: 8234487.
96. King J, Keim M, Teo R, Weening K, Kapur M, McQuillan K, et al. Genetic control of lithium sensitivity and regulation of inositol biosynthetic genes. *PLoS One.* 2010; 5(6):e11151. <https://doi.org/10.1371/journal.pone.0011151> PMID: 20567601.
97. Veltman DM, Lemieux MG, Knecht DA, Insall RH. PIP(3)-dependent macropinocytosis is incompatible with chemotaxis. *J Cell Biol.* 2014; 204(4):497–505. <https://doi.org/10.1083/jcb.201309081> PMID: 24535823; PubMed Central PMCID: PMC3926956.
98. Carnell M, Zech T, Calaminus SD, Ura S, Hagedorn M, Johnston SA, et al. Actin polymerization driven by WASH causes V-ATPase retrieval and vesicle neutralization before exocytosis. *J Cell Biol.* 2011; 193(5):831–9. <https://doi.org/10.1083/jcb.201009119> PMID: 21606208; PubMed Central PMCID: PMC3105540.
99. Veltman DM, Akar G, Bosgraaf L, Van Haastert PJ. A new set of small, extrachromosomal expression vectors for *Dictyostelium discoideum*. *Plasmid.* 2009; 61(2):110–8. <https://doi.org/10.1016/j.plasmid.2008.11.003> PMID: 19063918.
100. King J, Insall RH. Parasexual genetics of *Dictyostelium* gene disruptions: identification of a ras pathway using diploids. *Bmc Genetics.* 2003; 4. <https://doi.org/10.1186/1471-2156-4-12> PubMed PMID: WOS:000184659500001. PMID: 12854977
101. Arafah S, Kicka S, Trofimov V, Hagedorn M, Andreu N, Wiles S, et al. Setting up and monitoring an infection of *Dictyostelium discoideum* with mycobacteria. *Methods Mol Biol.* 2013; 983:403–17. https://doi.org/10.1007/978-1-62703-302-2_22 PMID: 23494320.

102. Gotthardt D, Dieckmann R, Blancheteau V, Kistler C, Reichardt F, Soldati T. Preparation of intact, highly purified phagosomes from *Dictyostelium*. *Methods Mol Biol*. 2006; 346:439–48. <https://doi.org/10.1385/1-59745-144-4:439> PMID: [16957306](#).
103. Fok AK, Clarke M, Ma L, Allen RD. Vacuolar H(+)-ATPase of *Dictyostelium discoideum*. A monoclonal antibody study. *J Cell Sci*. 1993; 106 (Pt 4):1103–13. Epub 1993/12/01. PMID: [8126094](#).
104. Journet A, Chapel A, Jehan S, Adessi C, Freeze H, Klein G, et al. Characterization of *Dictyostelium discoideum* cathepsin D. *Journal of cell science*. 1999; 112(21):3833–43.
105. Dieckmann R, von Heyden Y, Kistler C, Gopaldass N, Hausherr S, Crawley SW, et al. A myosin IK-Abp1-PakB circuit acts as a switch to regulate phagocytosis efficiency. *Mol Biol Cell*. 2010; 21(9):1505–18. Epub 2010/03/05. <https://doi.org/10.1091/mbc.E09-06-0485> PMID: [20200225](#); PubMed Central PMCID: [PMCPMC2861610](#).
106. Davidson AJ, King JS, Insall RH. The use of streptavidin conjugates as immunoblot loading controls and mitochondrial markers for use with *Dictyostelium discoideum*. *Biotechniques*. 2013; 55(1):39–41. <https://doi.org/10.2144/000114054> PMID: [23834384](#).
107. Sadosky AB, Wiater LA, Shuman HA. Identification of *Legionella pneumophila* genes required for growth within and killing of human macrophages. *Infect Immun*. 1993; 61(12):5361–73. PMID: [8225610](#); PubMed Central PMCID: [PMCPMC281323](#).
108. Feeley JC, Gibson RJ, Gorman GW, Langford NC, Rasheed JK, Mackel DC, et al. Charcoal-yeast extract agar: primary isolation medium for *Legionella pneumophila*. *J Clin Microbiol*. 1979; 10(4):437–41. PMID: [393713](#); PubMed Central PMCID: [PMCPMC273193](#).
109. Solomon JM, Rupper A, Cardelli JA, Isberg RR. Intracellular growth of *Legionella pneumophila* in *Dictyostelium discoideum*, a system for genetic analysis of host-pathogen interactions. *Infect Immun*. 2000; 68(5):2939–47. PMID: [10768992](#); PubMed Central PMCID: [PMCPMC97507](#).